Electronic Supplementary Material (ESI) for Chemical Communications

Oxidative C(sp^3)-H Bond Cleavage, C-C and C=C Coupling at a Boron Center with O_2 as Oxidant Mediated by Platinum(II)

Shrinwantu Pal, Peter Y. Zavalij, Andrei N. Vedernikov*

Department of Chemistry and Biochemistry, University of Maryland, College Park, MD 20742

E-mail: avederni@umd.edu

Index

D. NMR Spectra

E. X-Ray crystal structure determinations of [1]H·HCl, Na[6], 11 and 13

F. References

A. General Comments

All manipulations were carried out under purified argon using standard Schlenk and Glove-box techniques. All reagents for which syntheses is not given are commercially available from Aldrich, Acros or Pressure Chemicals and were used as received without further purification. PTFE-syringe filters were purchased from VWR and used as obtained. $Pt_2Me_4(SMe_2)_2$ and $PtPh_2(SMe_2)_2$ were prepared as described previously.[1] ^{1}H (500.132 MHz) and ^{13}C NMR (125.770 MHz) spectra were recorded on a Bruker Avance 500 spectrometer. ^{1}H NMR (400.132 MHz) spectra were recorded on a Bruker Avance 400 spectrometer. Chemical shifts are reported in ppm and referenced to residual protio-solvent resonance peaks. Coupling constants (represented as *J*=) indicate the ^{1}H-^{1}H coupling unless noted otherwise. ^{1}H NMR peaks corresponding to pyridine fragments in unsymmetrical complexes are assigned (as py or py'). However in many cases distinction between them could not be made, except in cases where Pt-coupling constants were influenced strongly by difference in the *trans*-influence of ligands. In such cases, appropriate assignments are noted. Elemental analyses were carried out by Columbia Analytical Services, Inc. ESI-MS were recorded on a JEOL AccuTOF-CS instrument using direct-injection technique, preventing exposure to O_2 and /or adventitious acid. ESI-MS were compared with mass envelopes for B and/or Pt –containing compounds and most intense peaks are reported. Formulas for solvent (THF) - containing sodium salts that we used to calculate their percent composition are deduced based on the intensity of the solvent (THF) signals observed in the ^{1}H NMR spectra of the same batch of the compound.

B. Synthetic Procedures

B1. Synthesis of 1,5-cyclooctanediyldi(2-pyridyl)borate, Na[1] (NaL)

Scheme 1

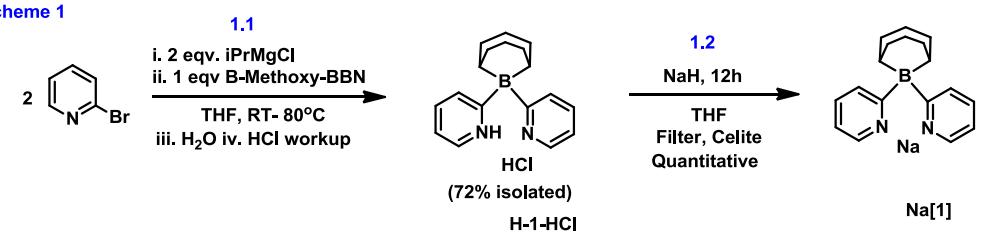

[1]H·HCl

2-pyridylmagnesium chloride was synthesized similar to Jäkle et al.[2] An air-free 250 mL round-bottom Schlenk flask was equipped with a stir-bar. To it 50 mL of dry THF and 4.3 mL of 2-bromopyridine (0.045 mole) were added. To this solution 22.5 mL of 2M isopropylmagnesium chloride (0.045 mole) was added dropwise with stirring, at room temperature. Immediately upon addition, the solution turned yellow. Stirring was continued for a period of 12h, over which, the solution gradually changed color from yellow to orange to wine-red. 18 mL of a 1M solution of 9-methoxy-9-borabicyclo[3.3.1]nonane in hexanes (0.018 mole) was added dropwise to it. The color immediately changed to light brown, followed by formation of copious amounts of precipitate within 10 minutes. The mixture was left to stir for 12h, followed by a 1-hour temperature increase to 80°C. During this period all precipitate dissolved, forming a greenish-brown solution. The mixture was stirred for a period of 24h at 80°C. The solution was then cooled down to room temperature and carefully transferred to a beaker containing 450 mL of ice water. Immediately upon contact with water, a tan precipitate developed with a yellow-brown supernatant solution. After 30 minutes of stirring the mixture was filtered through a medium fritted funnel. An excess of water is required to minimize loss of ligand dissolved in THF. The residue produced upon drying is a cream colored amorphous solid. The residue was washed with 100 mL of water followed by 100 mL of hexanes to aid in removal of organic byproducts. The filtrates were analyzed by ESI-MS and confirmed to contain a mixture of 2-bromopyridine, pyridine, and *B*-(2-pyridyl)-9-borabicyclo[3.3.1]nonane. The off-white residue was air-dried overnight to yield 11.2 g of an off-white solid. The solid is poorly soluble in THF, acetone and acetonitrile and but soluble in all of the above in the in the presence of 1 equivalent of acid. 3.0 g of the residue was suspended in 200 mL of dichloromethane and 25 mL of 10 M aqueous hydrochloric acid was added to it. The bilayer system was left to stir for a period of 5 hours. A yellow organic layer and a yellow aqueous layer formed. The organic layer was collected and the aqueous layer was extracted twice with 50 mL dichloromethane. The organic layers were combined, dried with anhydrous sodium sulfate, and stripped to dryness to yield 3.0 g of the target compound as a hydrogen chloride salt [**1**]H·HCl in virtually quantitative yield. Crystals suitable for XRD structure determination were obtained by dissolving 400 mg of [**1**]H·HCl in dichloromethane and vapor diffusion of pentane at 40°C.

^{1}H NMR (22°C, 500 MHz, DMSO-D_6, ppm) δ: 1.22 (br m, 2H), 1.47-1.70 (br m, 8H), 1.72-1.86 (m, 2H), 1.95 (br m, 2H, B-CH), 7.58 (t, 2H, *J*=6.8 Hz, py-5-CH), 8.01 (d, 2H, *J*=8.0 Hz, py-3-CH), 8.19 (t, 2H, *J*=7.4 Hz, py-4-CH), 8.53 (t, 2H, *J*=6.2 Hz, py-6-CH), 14.33 (br s, 2H, NH).

^{13}C NMR (22°C, 500 MHz, DMSO-D_6, ppm) δ: 19.9 (br m, B-CH), 24.1 (CH_2), 31.0 (CH_2), 122.4, 131.0, 140.5, 142.6 (pyridyl CH's), 180.2 (br m, pyridyl B-C).

ESI$^+$ MS of a solution of **1** in MeOH acidified with HBF_4: 279.19, Calculated 279.20.

Na[1]·2THF

3.0 g of [**1**]H·HCl was dissolved in 20 mL THF in a large vial inside a glove box. To it 1.0 g sodium hydride was carefully added with vigorous stirring. Vigorous evolution of hydrogen gas was observed. The color of the solution became light brown. Stirring was continued for another 8h. After this period, the solution was filtered through Celite, the residues washed with an additional 5 mL of THF in two portions. The combined filtrate was stripped to dryness and washed with hexanes to obtain 1.08 g of Na[**1**] in quantitative yield. The solvent of crystallization could not be removed even upon exposure of the product to high-vacuum for extended periods of time. Na**[1]** is extremely moisture sensitive, but stable in the presence of oxygen.

The ^{1}H and ^{13}C NMR spectra of this solid confirm its purity; this product was used for the preparation of platinum complexes without further purification.

<u>Attempted reaction with O_2</u>. A 15mg sample of Na**[1]** dissolved in a (0.4 mL CD_3OD : 0.2 mL THF-D_8) solution showed no change after a 4-day exposure to O_2.

^{1}H-NMR (22°C, 500 MHz, acetone-d_6, ppm) δ: 1.29 (br m, 2H), 1.52 (br m, 2H), 1.58-1.69 (br m, 4H), 1.78 (m, THF), 1.84-2.0 (m, 6H), 3.63 (m, THF), 6.61 (td, 2H, *J*=6.0, 1.4 Hz, py-5-CH), 7.22 (td, 2H, *J*=7.4, 1.9 Hz, py-4-CH), 7.45 (d, 2H, *J*=8.0 Hz, py-3-CH), 8.28 (d, 2H, *J*=4.7 Hz, py-6-CH).

^{13}C-NMR (22°C, 500 MHz, acetone-d_6, ppm) δ: 25.5-26.7 (br q, B-CH), 26.1 (free THF), 26.9 (Na-coordinated THF), 26.9 (CH_2), 33.4 (CH_2), 68.1 (free THF), 69.3 (Na-coordinated THF),117.3, 128.2, 133.2, 149.0 (pyridyl CH's), 192.8 (q, pyridyl B-C).

^{13}C-NMR (22°C, 500 MHz, DMSO-D_6, ppm) δ: 24.2(br q, B-CH), 25.1 (THF), 26.0 (CH_2), 32.4 (CH_2), 116.0, 126.7, 131.6, 147.8 (pyridyl CH's), 192.1-193.1 (q, pyridyl B-C).

ESI$^-$ MS of a solution of Na[**1**] in MeOH basified with $NaOCH_3$: 277.18, Calculated 277.19.

B2. Synthesis of Na[LPt^{II}Me$_2$], Na[2], and Na[LPt^{II}Ph$_2$], Na[3]

Scheme 2

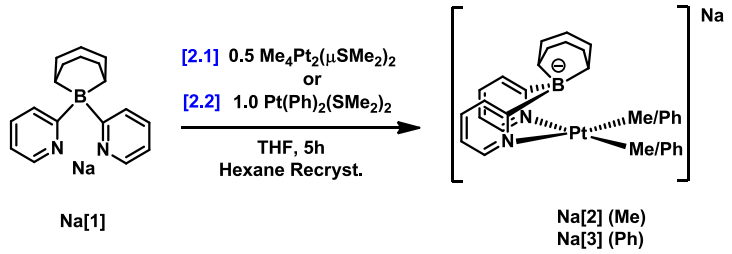

Na[2]·1.5THF: According to Scheme 2.1, 1.0 g (2.25 mmol) of Na[**1**] was dissolved in 10 mL THF in a reaction vial equipped with a stir bar. To the solution was added 0.646 g (1.125 mmol) of $Pt_2Me_4(\mu\text{-}SMe_2)_2$ with rapid stirring. The solution became light yellow in ten minutes. Stirring was continued for 5h with intermittent exposure to vacuum to facilitate removal of Me_2S. After this period, the solution was stripped to dryness to obtain a tan powder. The sample was recrystallized from a THF solution by precipitation with hexanes to yield 1.520 g of a tan colored powder, in 91% yield.

Complex Na[**2**] decomposes slowly at room temperature even if kept under Ar over long periods of time (2-3 days), and therefore must be stored in cold conditions. No decomposition was observed by ^{1}H NMR after 2 months when kept at -20 °C in a vial sealed under argon. Hence, no satisfactory elemental analysis could be produced. Purity of Na[**2**]·1.5THF was confirmed ^{1}H and ^{13}C NMR spectroscopy.

^{1}H NMR (22°C, 500 MHz, CD_3CN, ppm): 0.53 (s+Pt-satellites, $J_{Pt\text{-}H}$=82.4 Hz, 6H, $PtMe_2$), 1.29-1.46 (br m, 6H, BCH (1H), CH_2 (5H)), 1.68-1.90 (m, 10H, THF(6H), CH_2 (4H)), 2.41 (m+m, 2H, CH_2), 3.64 (m, 6H, THF), 4.43 (br m, 1H, BCH), 6.65 (vt, *J*=5.5, 1.7 Hz, 2H, py-5-CH), 7.34 (td, *J*=7.5, 1.7 Hz, 2H, py-4-CH), 7.45 (d, *J*=7.7 Hz, 2H, py-3-CH), 8.65 (d+Pt-satellites, $J_{Pt\text{-}H}$=26.4, *J*=5.9 Hz, 2H, py-6-CH).

^{13}C NMR (22°C, 500 MHz, CD_3CN, ppm): -20.0 (s+Pt-satellites, $J_{Pt\text{-}C}$=831 Hz, $PtMe_2$) 24.2 (q, B-CH), 26.4 (THF), 26.4 (CH_2), 29.2 (q, B-CH), 33.7 (CH_2), 33.8 (CH_2), 68.4 (THF), 119.4, 130.2, 132.2, 150.5 (pyridyl CH's), 190.2 (q, pyridyl B-C).

ESI$^-$ MS of a THF solution: 502.20, Calculated 502.20.

Na[3]·1.4THF: According to Scheme 2.2, 1.0 g (2.25 mmol) of Na[**1**] was dissolved in 10 mL THF in a reaction vial equipped with a stir bar. To the solution was added 1.06 g (2.25 mmol) of $PtPh_2(SMe_2)_2$ with rapid stirring. The solution became yellow in ten minutes. Stirring was continued for 5h with intermittent exposure to vacuum to facilitate removal of Me_2S. After this period, the solution was stripped to dryness to obtain a light-tan colored powder. The sample was recrystallized from THF-hexanes mixture to yield 1.68 g of a cream colored powder, analytically pure Na[**3**], in 94% yield.

Complex Na[**3**] is stable both in solution in THF-d_8, CD_3CN, and acetone-d_6 at room temperature if kept under Ar over long periods of time (2-3 days), and as a solid when stored under inert conditions. 1.4 mole of Na-bound THF could not be removed even upon extended exposure to high-vacuum but the signals of THF of the appropriate intensity were observed in its ^{1}H NMR spectra.

^{1}H NMR (22 °C, 500 MHz, CD_3CN, ppm) δ: 144-1.54 (br m, 3H, B(CH)+B(C*H*)(CH_2)), 1.70-1.88 (m, 11.6H, THF=5.6H, CH_2=6H), 1.96-2.06 (m, 2H, B(CH)(CH_2)), 2.43-2.55 (m+m, 2H, B(CH)(CH_2)), 3.58 (THF, 5.6H), 5.15 (br m, 1H, B(CH)), 6.52 (vt, *J*=5.5, 1.6 Hz, 2H, py-5-CH), 6.62 (tt, *J*=7.2, 1.5 Hz, 2H, Ph-p-CH), 6.78 (unresolved t, *J*=7.5 Hz, 4H, Ph-m-CH), 7.31 (td, *J*=7.6, 1.8 Hz, 2H, py-4-CH), 7.53 (d, *J*=7.9 Hz, 2H, py-3-CH), 7.57 (d+Pt-satellites, $J_{Pt\text{-}H}$=67, *J*=7.9 Hz, 4H, Ph-o-CH), 8.29 (d+Pt-satellites, $J_{Pt\text{-}H}$=27, *J*=5.9 Hz, 2H, py-6-CH).

^{13}C NMR (22 °C, 500 MHz, CD_3CN, ppm) δ: 23.7 (br m, B-CH), 26.4 (THF), 26.4 (CH_2), 31.8 (br m, B-CH), 33.7 (CH_2), 34.8 (CH_2), 68.4 (THF), 119.1, 120.9, 126.9 (s+Pt-satellites), 130.2, 133.4, 140.7, 150.3, 151.7 (s+unresolved Pt satellites), 190.3 (br m, pyridyl C-B).

ESI$^-$ of a THF solution of **Na[3]**: 626.22, Calculated 626.23.

Elemental Analysis (C, H, N): Calculated ($C_{30}H_{32}BN_2NaPt$·1.4THF): 56.98, 5.80, 3.73 Found: 57.38, 6.50, 3.37.

B3. Synthesis of Na[LPt^{II}Me(OMe)], Na[4], and Na[LPt^{II}Ph(OMe)], Na[5]

Scheme 3

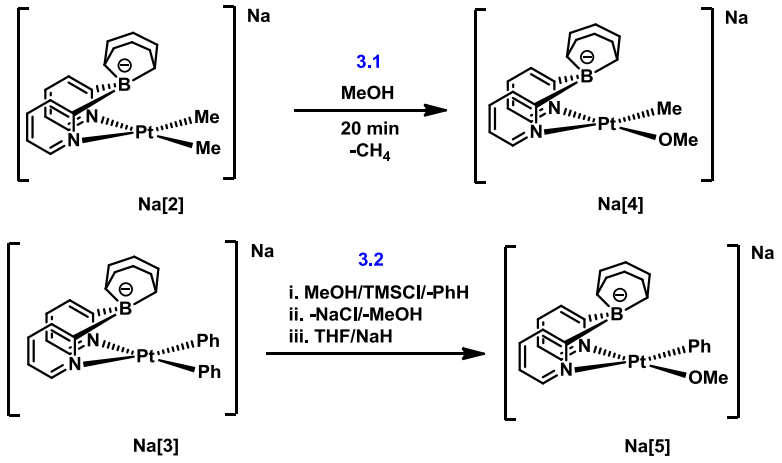

Na[4]. As shown in Scheme 3.1, 50 mg of Na[**2**] was taken in a stir-bar equipped reaction vial and 3 mL of methanol was added to it. Vigorous evolution of gas was seen. The entirety of the solid dissolved after 5 minutes, and stirring was continued for a period of 20 minutes. The contents of the vial were stripped to dryness, and a brown powder was obtained. The powder was washed with 1:1 v/v ether hexane mixture and exposed to high vacuum to obtain a yellow colored powder, Na[**4**]. The compound is stable in CD_3OD for at least 12 hours at RT and over long periods of time in CD_3CN in the absence of air or moisture.

Na[**4**] could not be isolated in analytically pure form even upon repeated crystallization from methanol or THF and was characterized in solution by ^{1}H, ^{13}C NMR and ESI-MS.

The ^{1}H and ^{13}C NMR spectra show a satisfactory purity of the sample used in our experiments.

^{1}H NMR (22°C, 500 MHz, THF-D_8, ppm) δ: 0.76 (s+Pt-satellites, 3H, J_{Pt-H}=70.9 Hz, PtMe), 1.28-2.00 (m, 11H, BCH(1H)+CH_2(10H)), 2.36-2.56 (m+m, 2H, CH_2), 3.50 (s+d, 3H, J_{Pt-H}=38 Hz, $PtOCH_3$), 4.67 (br, 1H, B-CH), 6.43 (vt, 1H, *J*=6 Hz, py-5-CH), 6.71 (vt, 1H, *J*=5.9 Hz, py'-5-CH), 7.23 (vt, 1H, *J*=7.2 Hz, py-4-CH), 7.30 (vt, 1H, *J*=6.8 Hz, py'-4-CH), 7.39 (d, 1H, *J*=7.5 Hz, py-3-CH), 7.51 (d, 1H, *J*=7.8 Hz, py'-3-CH), 8.47 (d+Pt-satellites, 1H, J_{Pt-H}=50.9, *J*=7.8 Hz, py-6-CH), 8.83 (d+unresolved Pt-satellites, 1H, *J*=5.1 Hz, py'-6-CH).

^{13}C NMR (22°C, 500 MHz, THF-D_8, ppm) δ: -19.2 (s+d, J_{Pt-C}=848 Hz, $PtCH_3$), 23.8 (br m, B-CH), 26.4 (CH_2), 26.4 (s, CH_2), 31.7 (br m, B-CH), 33.5 (CH_2), 33.6 (s, CH_2), 33.9 (s, CH_2), 34.4 (s, CH_2), 60.2 (s+unresolved Pt-satellites, $PtOCH_3$), 118.3, 119.4, 130.2, 130.28, 131.7, 132.8, 148.5, 152.5 (pyridyl CH's), 188.6 (q, pyridyl B-C), 191.50 (q, pyridyl B-C). Peak assignments were made by correlation with DEPT-45, 90 and 135 NMR spectra.

ESI$^-$ MS of a methanolic solution basified with sodium methoxide: 518.18, Calculated 518.19.

Na[5]·THF. As shown in Scheme 3.2, 200 mg of Na[**3**] (266 µmol) was dissolved in 3 mL of methanol in a reaction vial equipped with a stir-bar. In another vial, 34.0 µL (1 eqv.) of trimethylchlorosilane was dissolved in 1 mL of methanol and quantitatively transferred to the first vial containing **3** with rapid stirring. An additional 1 mL of methanol was used to complete the transfer. The solution was let to stir for a period of 5 minutes and rapidly stripped to dryness. During the process of evacuation, fine white precipitate of NaCl could be seen. Evacuation was completed in approx. 1h to obtain a tan colored powder. At this point, the entire solid was re-dispersed in 5 mL THF, cooled to -20 °C and 15 mg of sodium hydride was carefully added to the suspension with rapid stirring. Vigorous evolution of gas was observed and the mixture was let to stir for 10 minutes after which the contents were filtered through a PTFE–Syringe filter with an additional 1 mL of THF to aid in quantitative separation. The combined filtrates were stripped to dryness, and a light-tan colored powder was obtained.

Recrystallization of the entire solid from a THF solution by addition of hexanes and precipitation by cooling produced Na[**5**]. 1.0 mole of Na-bound THF could not be removed upon extended exposure to high-vacuum.

^{1}H NMR (22°C, 500 MHz, THF-D_8, ppm) δ: 1.38-1.52 (br m, 3H, CH_2(2H)+B-CH(1H)), 1.56-1.87(m, 10H, CH_2(6H)+THF(4H)), 1.88-2.03 (m, 2H, CH_2), 2.39-2.61 (m+m, 2H, CH_2), 3.43 (s+unresolved Pt-satellites, 3H, $PtOCH_3$), 5.05 (br m, 1H, B-CH), 6.26 (td, *J*=5.8, 1.8 Hz, py-5-CH), 6.69-6.78 (m, 2H, py'-5-CH+Ph-p-CH), 6.87 (t, 2H, *J*=7.4 Hz, Ph-m-CH), 7.17 (td, 1H, *J*=7.6, 1.7 Hz, py-4-CH), 7.31 (td, 1H, *J*=7.5, 1.7 Hz, py'-4-CH), 7.40 (d, 1H, *J*=7.8 Hz, py-3-CH), 7.49 (d, 2H, *J*=7.1 Hz, Ph-o-CH), 7.55 (d, 1H, *J*=7.7 Hz, py'-3-CH), 8.31 (d+Pt-satellites, 1H, $J_{Pt\text{-}H}$=44, *J*=6.1 Hz, py-6-CH, trans to PtPh), 8.80 (d+unresolved Pt-satellites, *J*=4.9 Hz, py'-6-CH, trans to $PtOCH_3$).

^{1}H NMR (22°C, 400 MHz, CD_3OD, ppm) δ: 1.35-1.55 (br m, 3H, CH_2(2H)+B-CH(1H)), 1.58-1.71 (br m, 2H, CH_2), 1.71-2.03 (br m+m+m, THF(1.9H)+CH_2(6H)), 2.37-2.60 (br m+m, 2H, CH_2), 3.2-3.4 (s+unresolved Pt-satellites, overlapping with CD_3OD signal), 3.72 (m, 1.9H, THF), 5.03(br m, 1H, BCH), 6.30 (td, 1H, *J*=5.6, 2.2 Hz, py-5-CH), 6.75 (vt, 1H, *J*=7.4 Hz, p-Ph), 6.8-6.9 (m, 3H, m-Ph(2H)+py(1H)), 7.23 (vt, 1H, *J*=8.1 Hz, py-CH), 7.30-7.50(m, 4H, o-Ph(2H)+Py(2H)), 7.55 (d, 1H, *J*=7.7 Hz, py-3-CH), 8.11 (d+Pt-satellites, *J*=6.8, $J_{Pt\text{-}H}$=49 Hz, py-6-CH, trans to OCH_3), 8.86 (d+unresolved Pt-satellites, *J*=5.4 Hz, py-6-CH, trans to PtPh).

^{13}C NMR (22°C, 500 MHz, THF-D_8, ppm) δ: 23.6 (br m, B-CH), 26.4 (CH_2), 26.4 (CH_2), 26.4 (THF), 32.3 (br m, B-CH), 33.7 (CH_2), 33.9 (CH_2), 34.5 (CH_2), 34.6 (CH_2), 60.1 (s+unresolved Pt-satellites, $PtOCH_3$) 68.3 (THF), 118.4, 119.1, 122.1, 127.0, 130.0, 130.2, 132.3, 133.4, 139.2, 147.2 (s+unresolved Pt-satellites), 149.2 (s+unresolved Pt-satellites), 153.7, 189.3 (br m, pyridyl B-C), 190.9 (br m, pyridyl B-C). A complex peak at 26.4 was cross checked for correct assignment by subtracting the integral corresponding to CH_2O- (of THF at 68.3 ppm) from the integral at 26.4 ppm. Such computation results in 68.3 set to 1C and 26.43 found to be 3C.

Elemental Analysis (C, H, N): Calculated ($C_{25}H_{30}BN_2NaOPt$·1.0THF): 51.56, 5.67, 4.15 Found: 51.31, 5.73, 4.07.

B4. Synthesis of Na[6] by oxidation of LPt^{II}Me(OMe), Na[4], and NaLPt^{II}Ph(OMe), Na[5], with O_2 in CH_3OH

Scheme 5

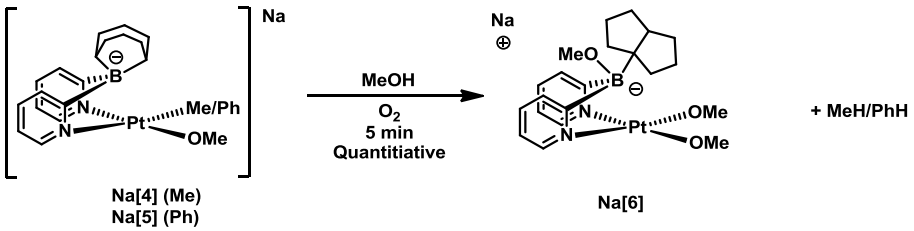

As shown in Scheme 5, 200 mg of Na[**4**] was dissolved in 4 mL methanol in a stir-bar equipped reaction vial in the glove box. The vial was taken out from the box and was exposed to O_2 with vigorous stirring. Stirring was continued for 10 minutes following which the mixture was stripped to dryness to yield a light yellow powder. The entirety of this solid was recrystallized from a 1 mL of THF solution by precipitation with hexanes to yield after drying 200 mg of analytically pure Na[**6**]·0.4THF (90 %). The residual Na-bound THF could not be removed even under high vacuum. The THF signals of the appropriate intensity were observed in its ^{1}H NMR spectra of this sample.

Crystals suitable for XRD were grown by layering a 100 mg sample of Na[**6**] dissolved in 3mL of THF with 2 mL of hexanes at -20 °C. According to the results of the X-ray structure determination, 1.25 mole of THF co-crystallized with Na[**6**].

Na[**6**] is unstable in the presence of even traces of acid or water but stable in the presence of excess base ($NaOCH_3$).

Na[**6**]·0.4THF:

^{1}H NMR (22°C, 400 MHz, CD_3CN, ppm) δ: 0.80-0.94 (br m, 3H, CH), 0.98-1.09 (br m, 3H, CH), 1.20-1.35 (br m, 4H, CH), 1.79 (m, 1.2H, THF), 2.56-2.78 (s+m, 3H+2H, B-OCH_3+CH), 3.25 (s unresolved Pt-satellites, 6H, $Pt(OCH_3)_2$), 3.63 (1.2H, THF), 4.22 (br sept, 1H, 3°C-H), 6.85 (td, 2H, *J*=6.7, 1.7 Hz, py-5-CH), 7.51 (td, 2H, *J*=7.9, 1.8 Hz, py-4-CH), 7.62 (d, 2H, *J*=7.7Hz, py-3-CH), 9.1 (d+unresolved Pt-satellites, 2H, *J*=5.7 Hz, py-6-CH), ipso-C not seen.

^{13}C NMR (22°C, 500 MHz, DMSO-d_6, ppm) δ: 25.7 (CH_2), 35.3 (CH_2), 39.1 (CH_2), 44.4 (CH), 46.2 (br, B-C), 51.6 (B-OCH_3), 58.7 ($PtOCH_3$), 119.8, 129.9, 132.1, 148.8 (pyridyl CH's), 179.9 (br m, pyridyl B-C).

^{13}C NMR (22°C, 500 MHz, THF-d_8, ppm) δ: 27.1 (CH_2), 36.7 (CH_2), 40.5 (CH_2), 46.2 (3°-CH), 52.4 (B-OCH_3), 59.7 ($Pt(OCH_3)_2$), 120.3, 131.6 (br), 132.7, 149.7, 182.6 (br m, pyridyl B-C). Peak assignments were made by correlation with DEPT-45, 90 and 135 NMR spectra.

ESI$^-$ MS of a methanolic solution basified with $NaOCH_3$: 564.18, Calculated 564.20.

Elemental Analysis (C, H, N): Calculated ($C_{21}H_{30}BN_2NaO_3Pt$·0.4THF): 44.05, 5.43, 4.55 Found: 44.05, 5.58, 4.48.

B5. Complete oxidation of Na[2] or Na[3] to form 10 or 11, respectively and bicyclo[3.3.0]oct-1(5)-ene, 9

Scheme 7

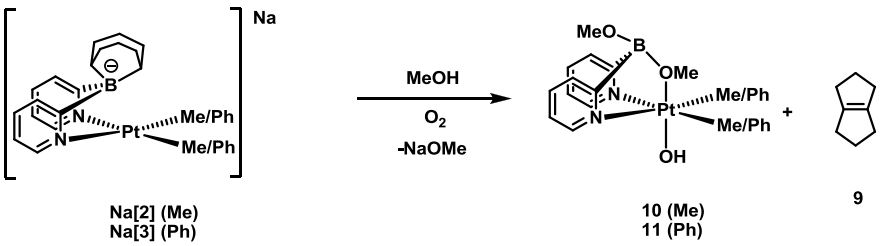

Oxidation of Na[2] to 10. 200 mg of Na[**2**] was dissolved in 1 mL of THF inside the glove-box. In a Schlenk tube equipped with a stir-bar, 4 mL of methanol was taken, cooled to -60 °C (dry-ice/Acetone) and O_2 was bubbled through it for 5 minutes. While continuing bubbling O_2, the 1 mL THF solution of Na[**2]** was added to it via a syringe. The dry-ice bath was removed and the solution was allowed to warm to room temperature over a period of 10 minutes, while continuing bubbling O_2. During this time a faint odor resembling 'alkenes' was found emanating from the reaction mixture. The solution in the Schlenk tube was stripped to dryness to yield a tan-colored powder. The contents were re-dispersed in 3 mL THF, 0.1 mL water was added to it, and the contents were stirred for 10 minutes. Fine white precipitate appeared along with the formation of a light-yellow solution. The contents were filtered through a PTFE-syringe filter and stripped to dryness to yield a powder. This powder was dissolved in 2 mL $CHCl_3$ and recrystallization was attempted by precipitation with hexanes to yield 158 mg of **10** (approx. 88% yield). Trace amounts of impurities, presumably due to unavoidable methanolysis and subsequent oxidation could be seen in the NMR.

^{1}H NMR (22°C, 400 MHz, $CDCl_3$, ppm) δ: 1.31 (br s, PtOH), 1.33 (s+Pt-satellites, 6H, J_{Pt-H}=69 Hz, $PtMe_2$), 3.04 (s+Pt-satellites, 3H, J_{Pt-H}=28 Hz, B-μ(OCH_3)-Pt), 3.57 (s, 3H, B-exo(OCH_3)), 7.11-7.16 (m, 2H, py-5-CH), 7.56-7.66 (overlapping-m, 4H, py-4-CH, py-3-CH), 8.57 (dt+Pt-satellites, 2H, J=5.3, 1.4 Hz, J_{Pt-H}≈16 Hz, py-6-CH).

Oxidation of Na[3] to 11

200 mg of Na[**3**] was dissolved in 5 mL methanol in a reaction vial equipped with a stir-bar inside the glove box and taken out. O_2 was bubbled through the solution for a period of 10 minutes. A characteristic 'alkene' smell was noticed. The solution changed from colorless to a faint yellow gradually. The solution was stripped to dryness, during the course of which fine precipitate started to appear. The sample was further dried to obtain a solid. Part of the solid was soluble in chloroform and part insoluble. The solid contents were re-dispersed in 3 mL $CHCl_3$, 0.2 mL water was added to the mixture and stirred for 10 minutes. As before, fine white precipitate and a light-yellow supernatant appeared. The supernatant was extracted with 2 mL chloroform in two more fractions, filtered through a PTFE-syringe filter and stripped to dryness to yield 142.6 mg of **11**, in 95% yield.

11 was recrystallized from a mixture of THF and hexanes at -20 °C, and fine colorless crystals of **11** suitable for X-ray diffraction were obtained. According to the results of the X-ray structure determination, 1.00 mole of THF co-crystallized with **11**. The THF could not be removed completely under vacuum. Residual THF signals were observed in the ^{1}H NMR spectra of this sample.

^{1}H NMR (22 °C, 500 MHz, $CDCl_3$, ppm) δ: 0.39 (br s, 1H, PtOH), 1.86 (m, 1.2H, THF) 3.33 (s+Pt-satellites, 3H, $J_{Pt\text{-}H}$=22.5 Hz, Pt-μ(OCH_3)B), 3.69-3.78 (s+m, 4H, B-OCH_3(3H), THF (1H)), 6.99-7.22 (m+m+td, 12H, $PtPh_2$+py-5-CH), 7.67 (td, 2H, *J*=7.34, 1.3 Hz, py-4-CH), 7.73 (d, 2H, *J*=7.45, py-3-CH), 8.68 (d+unresolved Pt-satellites, 2H, *J*=5.43, py-6-CH).

^{13}C NMR (22 °C, 500 MHz, $CDCl_3$, ppm) δ: 25.8 (THF), 51.9 (s+unresolved Pt-satellites, Pt-μ-(OCH_3)B), 55.4 (B-OCH_3), 68.2 (THF), 122.9, 125.1, 127.5 (s+unresolved Pt-satellites), 127.5, 129.6, 133.4, 137.0, 145.9, 171.1 (br m, pyridyl B-C).

Elemental Analysis (C, H, N): Calculated ($C_{24}H_{25}BN_2O_3Pt$·0.3THF): 49.06, 4.48, 4.54 Found: 49.10, 4.84, 4.28.

B6. Isolation and characterization of bicyclo[3.3.0]oct-1(5)-ene, 9:

In a separate experiment, 50 mg of Na[**3**] was oxidized in a manner similar to above, the methanolic solution was cooled to 0°C and extracted with 0.8 mL of cyclohexane-d_{12}. The cyclohexane extract was passed through a pipette packed with silica, and further filtered through a PTFE-syringe filter. The colorless solution was analyzed by ^{1}H and ^{13}C NMR, as well as GC-MS and found to match the mass of 108, corresponding to that of bicyclo[3.3.0]oct-1(5)-ene.

9:

^{1}H-NMR (22°C, 500 MHz, C_6D_{12}, ppm) δ: 2.10-2.16 (m, 8H, (C=C)C***H***), 2.18-2.25 (m, 4H, (C=C)CH_2C***H***).

^{13}C-NMR (22°C, 500 MHz, C_6D_{12}, ppm) δ: 29.3 (C=C-CH_2-***C***H_2), 30.0 (C=C-***C***H_2-CH_2), 146.5 (C=***C***-CH_2-CH_2).

GC-MS (EI): 108.

B7. Synthesis of $LPt^{IV}Me_3$, 13:

Scheme 8

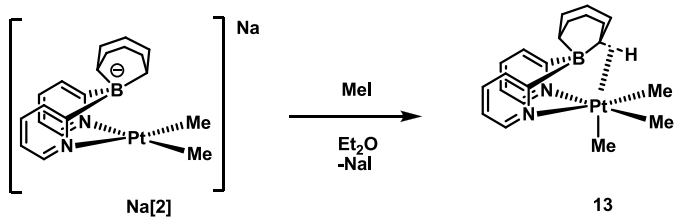

40 mg of Na[**2**] was dissolved in 5mL of ether in a reaction vial and 10 µL of methyl iodide (2 eqv.) was added to it. After 5 minutes of stirring, fine white precipitate could be seen. After a period of 20 minutes of stirring, the contents of the vial were filtered through a PTFE-Acrodisc filter and washed with an additional 2mL of ether. The filtrate was stripped to dryness to obtain 41 mg of a pale yellow flaky solid, **13**, in quantitative yield. **13** is stable in CD_3OD and under air at room temperatures. Heating in DMSO showed no signs of decomposition at temperatures up to 120 °C after 24 h.

X-ray quality crystals were obtained vapor diffusion of pentanes into a solution of 100 mg of **13** in 2 mL of dichloromethane at 40 °C.

13:

^{1}H NMR (22°C, 500 MHz, CD_2Cl_2, ppm) δ: -3.36 (br s+d, 1H, J_{Pt-H}=208 Hz, B-CH, agostic), 0.96 (s+d, 6H, $^2J_{Pt-C}$=65 Hz, $PtMe_2$, equatorial), 1.4 (s+d, 3H, $^2J_{Pt-C}$=81 Hz, PtMe, axial), 1.39-1.52 (m, 4H, CH_2), 1.62 (br m, 1H, B-CH), 1.73-1.87 (br m, 2H, CH_2), 1.89-1.97 (m, 2H, CH_2), 2.22-2.30 (m, 2H, CH_2), 7.0 (td, 2H, *J*=6.4, 1.8 Hz, py-5-CH), 7.55 (td, 2H, *J*=7.6, 1.7 Hz, py-4-CH), 7.59 (d, 2H, *J*=7.3 Hz, py-3-CH), 8.19 (d+Pt-satellites, 2H, J_{Pt-H}=18.1 Hz, *J*=5.9 Hz, py-6-CH).

^{13}C NMR (22°C, 500 MHz, CD_2Cl_2, ppm) δ: -10.4 (s+d, $^1J_{Pt-C}$=631 Hz, PtMe, equatorial), 2.0 (s+d, $^1J_{Pt-C}$=783 Hz, PtMe, axial), 22.0 (q, J_{C-B}=44 Hz, B-CH), 25.8 (CH_2), 31.5 (CH_2), 33.0 (CH_2, J_{Pt-C}=7.5 Hz), 56.1 (q, J_{C-B}=39 Hz, B-CH), 120.9 (s+d, J_{Pt-C}=20 Hz), 130.5, 135.5, 145.6 (s+d, J_{Pt-C}=20 Hz), 189.6 (q, J_{C-B}=49 Hz, pyridyl B-C).

Elemental Analysis (C, H, N): Calculated: 48.75, 6.04, 5.41, Found: 49.14, 5.92, 5.25.

B8. Preparation of Na[15] by reduction of 11 in CH_3OH with $NaBH_4$

25 mg of **11** (42 µmol) was dispersed in 2 mL of methanol. To this suspension was added 5mg $NaBH_4$. After stirring for 1h, the mixture was filtered through a PTFE syringe filter and the filtrate was stripped to dryness to obtain 30 mg of a tan colored solid. A ^{1}H-NMR and ESI-MS of the crude product confirmed the identity of Na[**15**]. Na[**15**] could not be obtained in analytically pure form owing to a large amount of $NaB(OCH_3)_4$ which could not be removed from the sample even after attempted recrystallization from THF: heptanes mixture or attempts to selectively extract Na[**15**] with various solvents.

Na[15]:

^{1}H NMR (22°C, 400 MHz, CD_3OD, ppm) δ: 3.35 (br, $B(OMe)_2$+), 6.6 (vt, *J*=7.2 Hz, 2H, p-Ph), 6.75 (m+m, 4H+2H, m-Ph+py-4-CH), 7.48-7.58(m+m, 6H, o-Ph+py-4-CH), 7.73 (d, 2H, *J*=8.6 Hz, py-3-CH), 8.43 (d+unresolved-Pt-satellites, 2H, py-6-CH).

ESI- (of CD_3OD solution): 578.18, Calculated: 578.16.

C. Reactivity and H/D exchange studies

C1. Reaction of Na[2] with CD_3OD to form Na[4-d_6]

10 mg of Na[**2**] was dissolved in CD_3OD in an NMR tube and a ^{1}H-NMR spectrum was recorded immediately. According to the NMR spectrum, complete conversion of Na[**2**] to Na[**4-*d*$_6$**] had occurred. Na[**4-*d*$_6$**] was not isolated from solution, but characterized by ^{1}H and ^{13}C NMR spectroscopy and ESI-MS.

Na[4-*d*$_6$]:

^{1}H NMR (22°C, 500 MHz, CD_3OD, ppm) δ: 1.27-1.44 (br, m, 3H, CH), 1.45-1.61 (br, m, 4H, CH), 1.66-1.82 (br, m, 4H*, CH, overlapping with THF), 2.32-2.53 (m=sept+sept, 2H, CH), 4.64 (br, 1H, B-CH), 6.53 (td, *J*=6.6, 1.6 Hz, 1H, py-5-CH), 6.80 (td, *J*=6.7, 1.5 Hz, 1H, py'-5-CH), 7.27 (td, *J*=7.8, 1.5 Hz, 1H, py-4-CH), 7.34 (td, *J*=7.6, 1.6 Hz, 1H, py'-4-CH), 7.38 (d, *J*=7.9 Hz, 1H, py-3-CH), 7.50 (d, *J*=7.6 Hz, 1H, py'-3-CH), 8.48 (d, $J_{Pt\text{-}H}$=33, *J*=6.1 Hz, 1H, py-6-CH), 8.76 (br, d, *J*=5.0 Hz, unresolved Pt-satellites, 1H, py'-6-CH). *Peak overlapping with THF was integrated by including THF signal and then subtracting from it the integral corresponding to the non-overlapping downfield THF signal.

^{13}C NMR (22°C, 500 MHz, CD_3OD, ppm) δ: 24.1 (br, B-CH), 26.5 (CH_2), 26.6 (CH_2, overlapping with THF), 32.7 (br m, B-CH), 33.7 (CH_2), 33.8 (CH_2), 34.2 (CH_2), 34.7 (CH_2), 119.2, 120.0, 130.6, 130.7, 132.6, 133.7, 150.5, 153.4, 188-193 (br+br, ipso-py-C).

ESI$^-$ of the NMR-solution basified with $NaOCD_3$: 524.22, Calculated 524.23

C2. Oxidation of Na[4] and Na[4-d$_6$] with O_2 in CD_3OD: Detection of CH_4 and CD_3H

Oxidation of Na[4]. 10 mg of Na[**4**] was dissolved in 0.5 mL of CD_3OD and a ^{1}H NMR was recorded. According to NMR, no deuteration of either Pt-bound CH_3 or OCH_3 groups had occurred. 1.1 eqv. of THF present in the sample was used as an internal standard to monitor product yields. 1.0 mL of CD_3OD was saturated with O_2 and the NMR-tube was completely filled with it, and shaken. A ^{1}H-NMR was recorded. On comparison of the two spectra, before and after oxidation, and calibrating the integrals with previously set value for THF, oxidation was found to have occurred cleanly to form Na[**6-*d$_6$***], in 96% yield by NMR . A very strong singlet at 0.21 ppm was visible, and assigned to methane. The Pt-bound OCH_3 did not exchange with OCD_3 of the solvent in the course of the reaction.

Oxidation of Na[4-*d*$_6$]. The contents of the NMR-tube obtained as mentioned in section C1 were frozen with liq. N_2 and the headspace of the NMR-tube was evacuated. O_2 was then admitted into the headspace at 30 psi pressure, the NMR-tube was sealed and the contents were thawed and shaken for homogeneity. An NMR was recorded quickly within 10 minutes of thawing. According to NMR, Na[**4-*d$_6$***] underwent complete oxidation to form Na[**6-*d$_9$***].

Observation of CD_3H upon oxidation of Na[4-*d*$_6$] in CD_3OD: In another similar experiment, to a 0.2mL solution of Na[**4-*d$_6$***] in CD_3OD was added O_2-saturated CD_3OD, taking care to fill the entire headspace of the NMR tube. The NMR tube was sealed and a ^{1}H-NMR spectra was recorded. A septet at 0.15 ppm, corresponding to CHD_3 was observed, in addition to signals corresponding to Na[**6-*d$_9$***].

Na[6-*d*$_9$]:

^{1}H NMR (22°C, 500 MHz, CD_3OD, ppm) δ: 0.85-0.94 (br, sept, 2H, CH), 1.03-1.11 (br, sept, 2H, CH), 1.17-1.25 (br, quint, 2H, CH), 1.26-1.44 (br, m+m, 4H, CH), 2.42-2.53 (br, m, 2H, CH), 4.73 (br, sept, 1H, 3°CH), 6.94 (td, *J*=6.7, 1.6 Hz, 2H, py-5-CH), 7.56 (vt, *J*=7.5 Hz, 2H, py-4-CH), 7.64 (d, *J*=7.9 Hz, 2H, py-3-CH), 8.82 (d, *J*=6.0 Hz, 2H, unresolved Pt-satellites, py-6-CH). Residual THF signals not reported.

^{13}C NMR (22°C, 500 MHz, CD_3OD, ppm) δ: 27.1 (CH_2), 36.9 (CH_2), 40.4 (CH_2), 46.8 (3°-CH), 121.4, 133.9, 131.8, 151.6, 181.2 (br m, ipso-py-C). Residual THF signals not reported.

ESI$^-$ of the NMR solution basified with $NaOCD_3$: 573.23, Calculated 573.26.

C3. In-situ preparation of Na[3-d_{10}]: H/D exchange between $CD_3OD/LPt^{II}Ph_2$ and $CD_3OH/LPt^{II}(C_6D_5)_2$

35 mg of Na[**3**] was dissolved in 0.6 mL CD_3OD and a ^1H NMR was recorded immediately. The spectrum was consistent with the presence of two Pt-bound phenyl groups and a C_s symmetrical structure. The solution was monitored by ^1H NMR periodically every hour. The signals corresponding to the protons of the $PtPh_2$ moiety were found to gradually decrease in intensity and after 8h, complete deuteration of the $PtPh_2$ moiety was observed. The solution was then transferred to a vial equipped with a stir-bar and the solvent was stripped off under vacuum. An off-white solid similar in appearance to the starting material was observed. The solid was dissolved in 0.6 mL CD_3OH and periodically monitored by ^1H-NMR (with suppression of the OH signal) for reappearance of the aforesaid signals. The sample underwent complete H/D exchange after a period of 4h.

Na[3], immediately after dissolution in CD_3OD:

^1H NMR (22°C, 500 MHz, CD_3OD, immediately after dissolution, ppm) δ: 1.42-1.56 (m, 3H, CH_2+CH), 1.73-1.90 (m+m, 11H, THF=5H, CH_2=6H), 1.93-2.06 (m, 2H, CH_2), 2.44-2.57 (m, 2H, CH_2), 3.71 (m, 5H, THF), 4.73-4.80 (br, 1H, CH), 6.48 (vt, 2H, *J*=5.5, 1.5 Hz, py-5-CH), 6.64 (vt, 2H, *J*=7.2 Hz, Ph-p-CH), 6.78 (vt, 4H, *J*=7.6 Hz, Ph-m-CH), 7.26 (td, 2H, *J*=7.6, 1.7 Hz, py-4-CH), 7.51 (d, 2H, *J*=8.0Hz, py-3-CH), 7.63 (d+Pt-satellites, 4H, $J_{Pt\text{-}H}$=62.0 Hz, *J*=7.1 Hz, Ph-o-CH), 8.24 (d+unresolved Pt-satellites, 2H, *J*=5.6 Hz, py-6-CH).

Na[3-d_{10}], 8h after dissolution in CD_3OD:

^1H NMR (22°C, 500 MHz, CD_3OD, 8h after dissolution, ppm) δ: 1.42-1.56 (m, 3H, CH_2+CH), 1.73-1.90 (m+m, 11H, THF=5H, CH_2=6H), 1.93-2.06 (m, 2H, CH_2), 2.44-2.57 (m, 2H, CH_2), 3.71 (m, 5H, THF), 4.73-4.80 (br, 1H, CH), 6.48 (vt, 2H, *J*=5.5, 1.5 Hz, py-5-CH), 7.26 (td, 2H, *J*=7.6, 1.7 Hz, py-4-CH), 7.51 (d, 2H, *J*=8.0Hz, py-3-CH), 8.24 (d+unresolved Pt-satellites, 2H, *J*=5.6 Hz, py-6-CH). Peaks corresponding to $PtPh_2$ moiety silent.

^{13}C NMR (22°C, 500 MHz, CD_3OD, 8h after dissolution, ppm) δ: 23.7 (br m, B-CH), 26.6 (THF), 26.9 (CH_2), 33.50-34.7 (br m, B-CH), 34.0 (CH_2), 35.0 (CH_2), 69.0 (THF), 118.9 (s+Pt-satellites, $J_{Pt\text{-}C}$=22 Hz, py-CH), 130.2 (s+unresolved Pt-satellites, py-CH), 133.3 (py-4-CH), 152.5 (s+Pt-satellites, $J_{Pt\text{-}C}$=34.7 Hz, py-6-CH), 190.7-192.2 (br m, py-ipso-C).

ESI^- MS of a methanolic solution of Na[**3-d_{10}**]: 636.28, Calculated 636.29.

C4. Preparation of Na[5-d_8]

A 0.5 mL CD_3OD solution containing 50 mg of **Na[3]** in a vial was let stir for 10h to convert it to Na**[3-d_{10}]** via complete deuteration of the $PtPh_2$ fragments, as mentioned in section C2. Following a procedure identical to that mentioned in section B3, 9 µL (1 eqv.) of trimethylchlorosilane in 0.5 mL CD_3OD was added and immediate formation of precipitate was observed. After 10 minutes of further stirring, the mixture was stripped to dryness. To this mixture was added 2 mL THF followed by addition of 5 mg NaH. The suspension was filtered quickly and stripped to dryness to obtain a brown solid. Although trace impurities were visible in the ^{1}H-NMR spectrum in CD_3OD, the major species was identified as Na[**5-d_8**] by comparison with the ^{1}H-NMR spectrum of analytically pure Na[**5**], as obtained in section B3, in CD_3OD. Yields were not determined owing to multi-step conversions/filtrations involving minute quantities.

^{1}H NMR (22°C, 400 MHz, CD_3OD, ppm) δ: 1.35-1.55 (br, m, 3H, CH_2(2H)+B-CH(1H)), 1.55-2.04 (17H, CH_2(8H)+THF(9H)), 2.37-2.60 (br, m+m, 2H, CH_2), 3.72 (m, 9H, THF), 5.03(br, 1H, BCH), 6.30 (td, 1H, *J*=5.6, 2.2 Hz, py-5-CH), 6.84 (vt, 1H, py-CH), 7.23 (vt, 1H, *J*=7.9 Hz, py-CH), 7.36 (vt, 1H, *J*=7.7 Hz, py-CH), 7.55 (d, 1H, *J*=7.8 Hz, py-3-CH), 8.11 (d+Pt-satellites, *J*=6.8, $J_{Pt\text{-}H}$=49 Hz, py-6-CH, trans to OCH_3), 8.86 (d+unresolved Pt-satellites, *J*=5.4 Hz, py-6-CH, trans to PtPh). Peak assignments were made with respect to ^{1}H-NMR spectrum of Na[**5**] in CD_3OD, section B3.

C5. Oxidation of Na[5] and Na[5-*d*$_8$] with O_2 in CD_3OD: Detection of C_6H_5 and C_6D_5H

Oxidation of Na[5]: 25 mg of Na[**5**] was dissolved in 0.6 mL CD_3OD in a sealable NMR-tube inside the glove box and a ^{1}H NMR was recorded. According to NMR, no deuteration of either Pt-bound C_6H_5 or OCH_3 fragments had occurred. The contents of the NMR-tube were then frozen, the headspace was evacuated and refilled with 30 psi O_2 and the NMR tube was sealed. The contents were thawed, the NMR tube was shaken for homogeneity and a ^{1}H NMR was recorded within 10 minutes of thawing. According to NMR, as in the case of Na[**4**], complete oxidation of Na[**5**] was observed along with the formation of 1 equivalent of benzene. The amount of benzene produced was quantified using signals of the THF present in Na[**5**] as an internal standard.

Oxidation of Na[5-*d*$_8$]: A partially deuterated complex Na[**5-*d*$_8$**] (c.f. section C4) was oxidized similarly in a NMR tube in CD_3OD and a ^{1}H NMR was recorded. One singlet at 7.16 ppm integrating to 1H (with THF as an internal standard) in the ^{1}H NMR spectrum confirmed the formation of C_6D_5H. Some unassigned decomposition was also seen.

C6. Oxidation of Na[2] with O_2-saturated CD_3OD

Oxidation of Na[2]: 5 mg of solid Na[**2**] containing 2.5 moles THF/mole complex was charged in an NMR-tube and placed at -60°C in a dry-ice/acetone bath. 0.8 mL of CD_3OD was cooled to -60°C in a vial and O_2 was bubbled through it for a period of 10 minutes and quickly transferred to the NMR-tube. The NMR-tube was sealed, shaken and a ^{1}H-NMR was recorded within 5 minutes. According to NMR, based on THF-internal standard, the yields of **10-*d*$_7$** and bicyclo[3.3.0]oct-1-ene were 92% and 94% respectively (c.f. NMR spectra). Yield for **10-*d*$_7$** was computed by averaging the integrations of the aromatic signals over 8 units (theoretical maximum). Partial D-incorporation into the $PtMe_2$ fragment could not be avoided. The identity of **10-*d*$_7$** was additionally confirmed by ESI-MS of the NMR-solution.

10-*d*$_7$:

^{1}H NMR (22°C, 400 MHz, CD_3OD, ppm) δ: 1.44 (s+multiplets+Pt-satellites, 4.7H, $J_{Pt\text{-}H}$=68.4 Hz, $Pt(CH_{(3-n)}D_n)_2$), 1.87 (m, THF, internal-std, 10H), 2.08-2.29 (m+m, 11.36 H, bicycloocetene), 3.73 (m, THF, internal-std, 10H), 7.32 (ddd, 1.84H, *J*=5.4, 1.5 Hz, py-5-CH), 7.70 (d, 1.72H, *J*=7.5 Hz, py-3-CH), 7.80 (td, 1.89H, *J*=7.6 Hz, py-4-CH), 8.65 (d+unresolved Pt-satellites, 1.91H, *J*=5.5 Hz, py-6-CH).

ESI$^+$-MS of CD_3OD solution, **10-*d*$_7$**·H: 485.23, Calculated: 485.21

C7. Stepwise oxidation of NaLPt^{II}Ph$_2$, Na[3] with O$_2$ and detection of Na[8-*d*$_3$]

Scheme 6

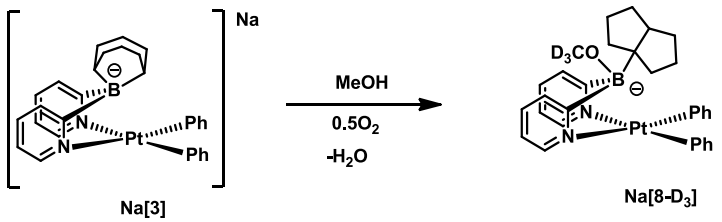

As shown in Scheme 3, 15 mg of Na[**3**] was dissolved in 0.6 mL of CD_3OD in a sealable NMR tube and 0.25 mL of O_2 (~0.5eqv. at RTP) taken in a syringe was slowly bubbled through the solution from the bottom of the NMR tube with a long needle. The tube was quickly sealed and shaken for 10 minutes. A ^{1}H NMR spectrum was recorded after this time. According to NMR, According to NMR, and based on THF as internal standard, Na[**8-*d*$_3$**] was formed in 94% yield, along with the formation of 6.5% of bicyclooctene, **9**, and 6.5% of **11-*d*$_7$** (c.f. NMR spectra). The characteristic signature of the B-bound bicyclo[3.3.0]octyl fragment, similar to that of previously characterized Na[**6**], is clearly seen in the ^{1}H-NMR spectrum. An aliquot was analyzed by ESI-MS and a peak at 659.26 confirmed the identity of Na[**8-*d*$_3$**]. Na[**8-*d*$_3$**] was characterized by ^{1}H-NMR and ESI-MS only for mechanistic proof-of-concept and no attempts were made towards isolating it.

The oxidation of Na[**3**] was completed by bubbling about 1.0 mL O_2 through the remaining solution in the NMR-tube and it was found to convert to **11-*d*$_7$** and **9** in 91% yield.

Na[8-*d*$_3$]:

^{1}H NMR (22°C, 400 MHz, CD_3OD, ppm) δ: 0.93-1.02 (m, 2H, CH_2), 1.09-1.18 (m, 2H, CH_2), 1.21-1.31 (m, 2H, CH_2), 1.32-1.50 (m+m, 4H, CH_2), 2.45-2.57 (m, 2H, CH_2), 4.74 (complex-septet, 1H, BCC***H***), 6.53-6.64 (m, 4H, py-5-CH(2H)+Ph(2H)), 6.67-6.79 (m, 4H, py-4-CH(2H)+Ph(2H)), 7.34-7.54 (m, 6H, Ph), 7.79 (d, 2H, *J*=8.2 Hz, py-3-CH), 8.37 (d+unresolved Pt-satellites, 2H, py-6-CH).

ESI$^-$ MS of CD_3OD solution basified with $NaOCD_3$: 659.27, Calculated: 659.26.

C8. Oxidation of Na[3] in CD$_3$OD by H$_2$O$_2$

14 mg of Na[**3**] was dissolved in a mixture of 0.3 mL of CD_3OD and 03. THF-*d*$_8$ in a NMR tube and a ^{1}H-NMR spectrum was recorded. The THF signal was used as internal standard. 6 µL of 30% aq. H_2O_2 was added to the NMR tube and shaken, and a ^{1}H-NMR NMR spectrum was recorded immediately. According to the NMR, based on THF integration, Na[**3**] was completely oxidized to **12**-*d*$_7$ (90% yield) and **10** (90% yield).

C9. Oxidation of NaLPt^{II}Ph$_2$, Na[3] and NaLPt^{II}Me(OMe), Na[4] in the presence of TEMPO

Oxidation of 3. 15 mg of solid Na[**3**] (20.0 µmol) was added to a vial with 6 mg (2 eqv.) solid TEMPO radical. To this vial was added 0.6 mL of CD_3OD and stirred for 2 minutes to obtain an orange colored solution. A ^{1}H-NMR was recorded and found to be a match to that of Na[**3**], i.e. no reaction between Na[**3**] and TEMPO was observed. The peaks were broadened significantly, however, no difference in chemical shifts was observed. This solution was oxidized by bubbling O_2 through the tube for a period of 10 minutes. After this period, according to ^{1}H NMR, all starting material had converted to **11-*d*$_7$** and **9**. Analysis of the HBF_4 – acidified reaction mixture above by means ESI-MS did not reveal formation of any TEMPO adducts as well.

Oxidation of 4. 15 mg of Na[**4**] (27.7 µmol) in the presence of 6 mg (2 eqv.) TEMPO radical in CD_3OD was performed identical to above, except O_2 was bubbled for a period of 2 minutes. According to ^{1}H-NMR, oxidation was found to have occurred cleanly, and spectral match confirmed the identity of Na**[6-*d*$_6$]**. Signals were significantly broadened due to the presence of TEMPO. Analysis of the HBF_4 – acidified reaction mixture above by means ESI-MS did not reveal formation of any TEMPO adducts as well.

C10. Oxidation of Na[3] and Na[4] with $^{18}O_2$ in methanol

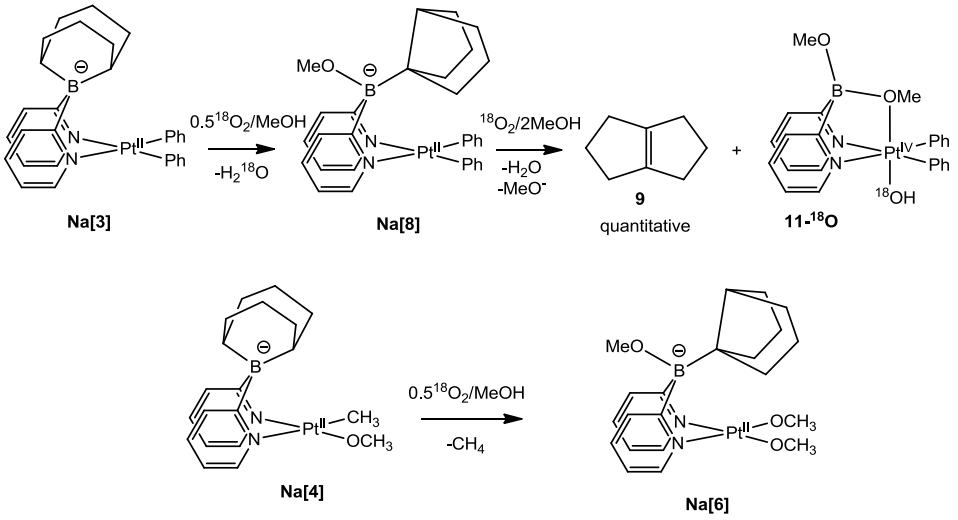

A sample of 10 mg of Na[**3**] was oxidized under 1 atm of $^{18}O_2$ and the methanolic solution was analyzed by ESI-MS (positive mode).
ESI$^+$ of methanolic solution of **11-^{18}O** acidified with 10% HBF_4: **11-^{18}O·H$^+$**: 598.16, Calculated: 598.17.
Similarly, a sample of Na[**4**] was oxidized under 1 atom of $^{18}O_2$ in methanol, and an ESI-MS (negative mode) was recorded.
ESI$^-$ of methanolic solution of Na[**6**]: 518.18, Calculated 518.19.
Thus, according to ESI-MS one ^{18}O atom was incorporated in **11** but none in Na[**6**].

C11. Reduction of 11 with $NaBH_4$ in CD_3OD to form Na[15-d_{16}] and comparison to direct oxidation of Na[3-d_{10}] to 12-d_{17} with O_2

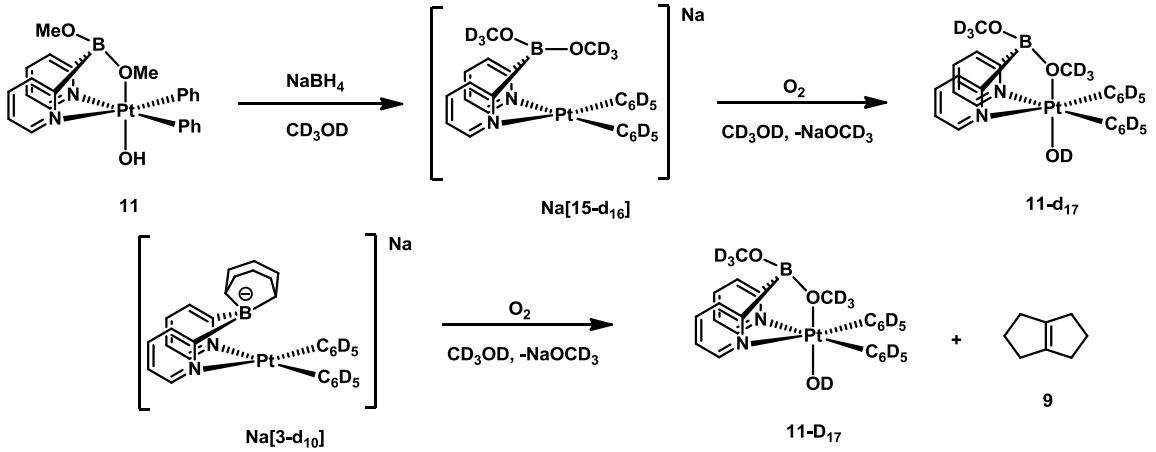

C11.1. Reduction of 11 to Na[15-d_{16}]. A sealable NMR-tube was charged with 15mg of **11** (25.2 µmol) and 3 mg $NaBH_4$ (79.3 µmol). To this was added 0.7 mL of CD_3OD cooled to -20°C and the NMR-tube was shaken. Slow bubbling and formation of trace amounts of Pt-black was seen. The reaction mixture was monitored by ^{1}H-NMR using THF present in the sample as internal standard and reaction was found to be complete in 90 minutes. According to NMR, 83% of all starting material was converted to Na[**15-*d*$_{16}$**]. The mixture was then filtered through a PTFE-syringe filter to obtain a clear light-yellow filtrate. An ESI-MS (negative mode) was recorded using 0.1 mL aliquot of the filtrate. The rest of the filtrate was saved in an NMR tube for the purpose of oxidation.

Na[15-d_{16}] ^{1}H NMR (22°C, 400 MHz, CD_3OD, ppm): δ: 6.74 (td, 2H, *J*=5.8, 1.8 Hz, py-5-CH), 7.50 (td, 2H, *J*=7.2, 1.8 Hz, py-4-CH), 7.7 (d, *J*=7.8 Hz, py-3-CH), 8.4 (d+unresolved Pt-satellites, 2H, py-6-CH)

ESI$^-$ (of CD_3OD solution): 594.19, Calculated: 594.16

C11.2. Oxidation of Na[15-*d*$_{16}$] to 11-*d*$_{17}$. O_2 was bubbled through the NMR solution obtained from (A) for a period of 10 minutes and an NMR was recorded. According to NMR, **11-*d*$_{17}$** was formed in 83% yield. Some benzene was seen in the NMR spectrum. ESI-MS was recorded of the filtrate.

ESI$^+$ (of CD_3OD solution): **11-*d*$_{17}$**·H: 612.19, Calculated: 612.17

C11.3. Direct oxidation of Na[3-*d*$_{10}$] to 11-*d*$_{17}$ and 9. 15 mg of Na[**3**] was dissolved in CD_3OD and stored in a sealed NMR-tube for 8h as mentioned before (c.f. section 3) After 8h a ^{1}H-NMR was recorded to confirm complete deuteration of the $PtPh_2$ fragment. At this point, O_2 was bubbled through the solution for a period of 10 minutes and a ^{1}H-NMR was recorded. According to NMR, complete conversion of Na[**3-*d*$_{10}$**] to **11-*d*$_7$** had occurred and the spectra was found to be a match with the product of oxidation of Na[**15-*d*$_{16}$**] viz. **11-*d*$_{17}$**. Signals corresponding to bicyclo[3.3.0]oct-1-ene were found to match to those observed in the experiment where Na**[3]** was oxidized prior to deuteration of the $PtPh_2$ fragment.

C12. Catalytic aerobic oxidation of $NaBH(OMe)_3$ and $NaBH_4$ in CD_3OD by 11

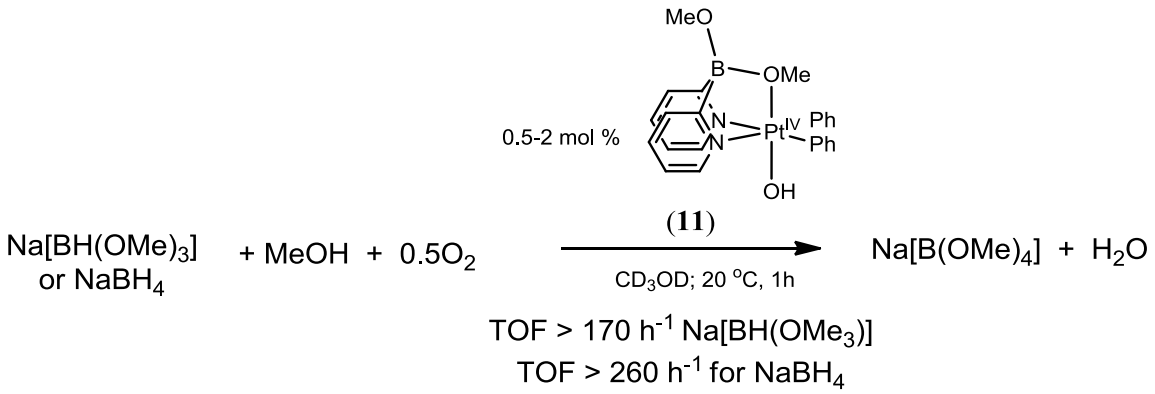

<u>Oxidation of Na[BH(OMe)$_3$]</u> (50.0 mg; 0.391 mmol) was performed with 0.5, 1.0, and 2.0 mole % catalyst **12** loading in 0.8 mL CD_3OD with THF as internal standard. Catalyst was weighed out, dissolved in 0.3 mL CD_3OD and appropriate amount of $NaBH(OMe)_3$ (see Table below) as a solution in 0.3 mL CD_3OD were combined under argon atmosphere. Oxygen gas was admitted into the reaction mixture which was stirred vigorously in a 5 mL Schlenk flask. An ^1H NMR spectrum was recorded before introducing O_2 and after 1h of the reaction. The decrease in the integral intensity corresponding to the BH fragment of $[BH(OMe)_3]^-$ (q+sept., -0.18 ppm) matched the increase in the CD_3O*H* signal intensity. A similar experiment was performed in the absence of O_2 to correct for the slow background methanolysis and the H/D exchange of the BH fragment.

<u>Oxidation of $NaBH_4$</u> was similarly performed. A stock solution of 76 mg catalyst in 3 mL CD_3OD containing THF as internal standard was prepared, appropriate amounts of this solution was added to a 5 mL Schlenk flask containing 5mg (0.132 mmol $NaBH_4$), with added 14.2 mg of NaOMe in each run to suppress protonolysis of $NaBH_4$.
A similar experiment was performed in the absence of O_2 to correct for the slow background methanolysis and the H/D exchange of the BH fragment.

The TOF of at about 178/hour was observed for $Na[BH(OMe)_3]$ with 0.5 mole % catalyst loading and 216/hour for $NaBH_4$ with 1.66 mole % catalyst loading.

Table 1S. The catalytic performance of complex **11** in the oxidation of $Na[BH(OMe)_3]$ with O_2 (1 atm) in 0.8 mL CD_3OD at 22 ^oC; reaction time is 1.0 hour.

#	$Na[BH(OMe)_3]$, mg	Catalyst **11**, mole %	Conversion of $Na[BH(OMe)_3]$, %	TON
1	50.0	-	3.2	-
2	100.0	0.5	92.2	178[a]
3	50.0	1.0	100	97[a]
4	50.0	2.15	100	45[a]

[a] The value is corrected for the contribution of the background reaction.

Table 2S. The catalytic performance of complex **11** in the oxidation of $NaBH_4$ with O_2 (1 atm) in 0.6 mL CD_3OD at 22 ^oC; reaction time is 1.0 hour.

#	$NaBH_4$, mg	Catalyst **11**, mole %	NaOMe added	Conversion of $NaBH_4$, %	TON
1	5	-	14.2	10.1	-
2	5	1.66	14.2	100	216[b]
4	5	5	14.2	100	71.9[b]

[b] The value is corrected for the contribution of the background reaction, TONs reported are based on 4 oxidizable Hydrides in $_{NaBH4}$

D. NMR spectra

D1

1H.HCl

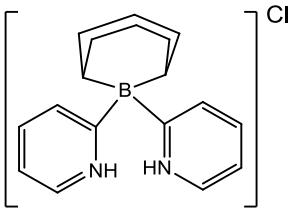

^{1}H NMR spectrum of [**1**]H_2Cl in DMSO-d_6 (22°C, 500.132 MHz); CH_2Cl_2 (5.76 ppm) is a reference

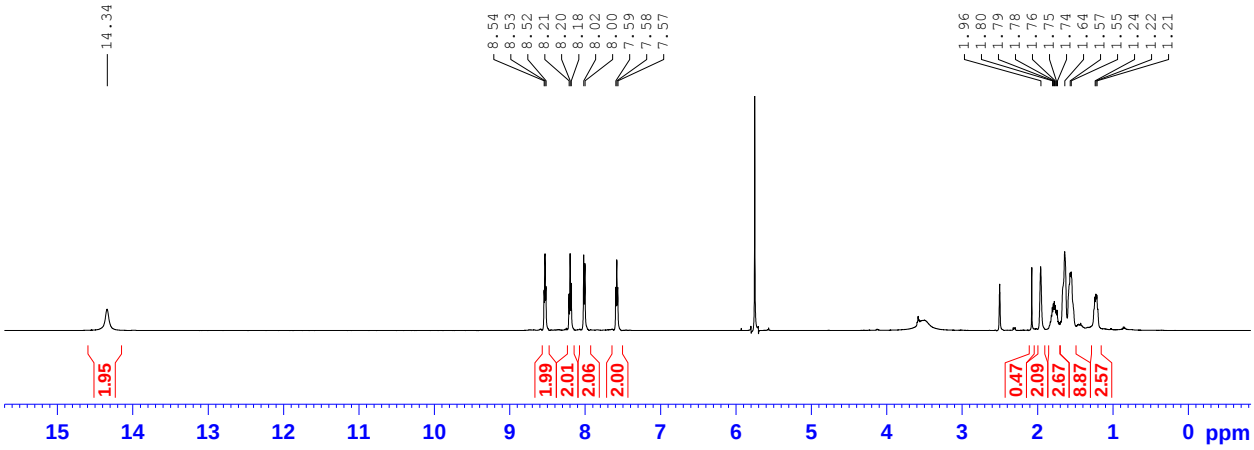

^{13}C NMR spectrum of [**1**]H_2Cl in DMSO-d_6 (22°C, 125.769 MHz); CH_2Cl_2 (54.91 ppm) is a reference

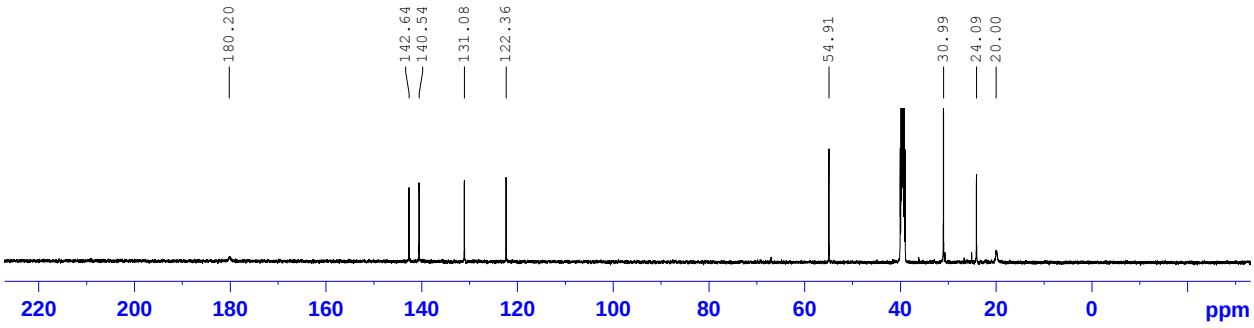

D2

Na[1]-2THF

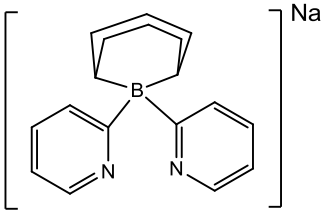

^{1}H NMR spectrum of Na[**1**]·2THF in acetone-d_6 (22°C, 500.132 MHz)

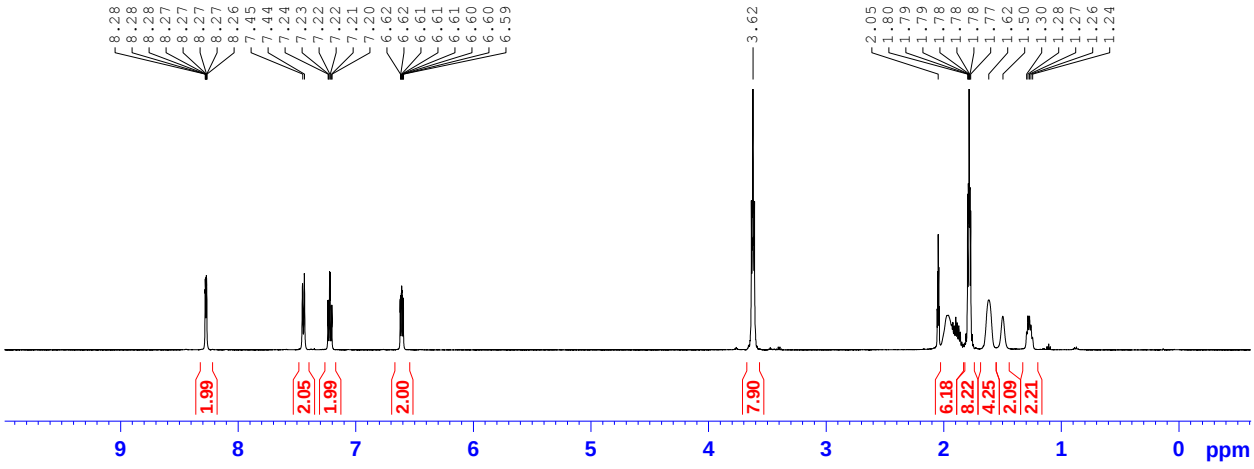

^{13}C NMR spectrum of Na[**1**]·2THF in acetone-d_6 (22°C, 125.769 MHz). Free THF (26.2, 68.1) and Na-bound THF (26.9, 69.3) produce two sets of signals.

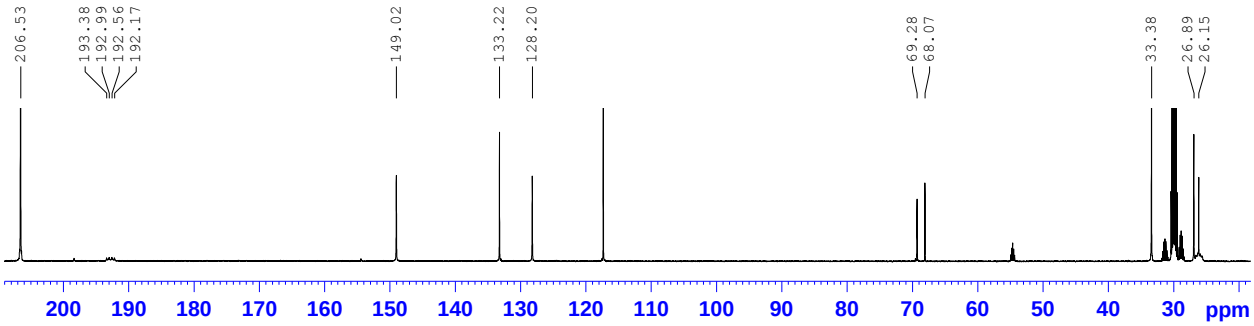

D3

Na[2]

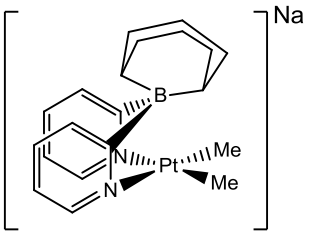

^{1}H NMR spectrum of Na[**2**]·1.5THF in CD_3CN (22°C, 500.132 MHz)

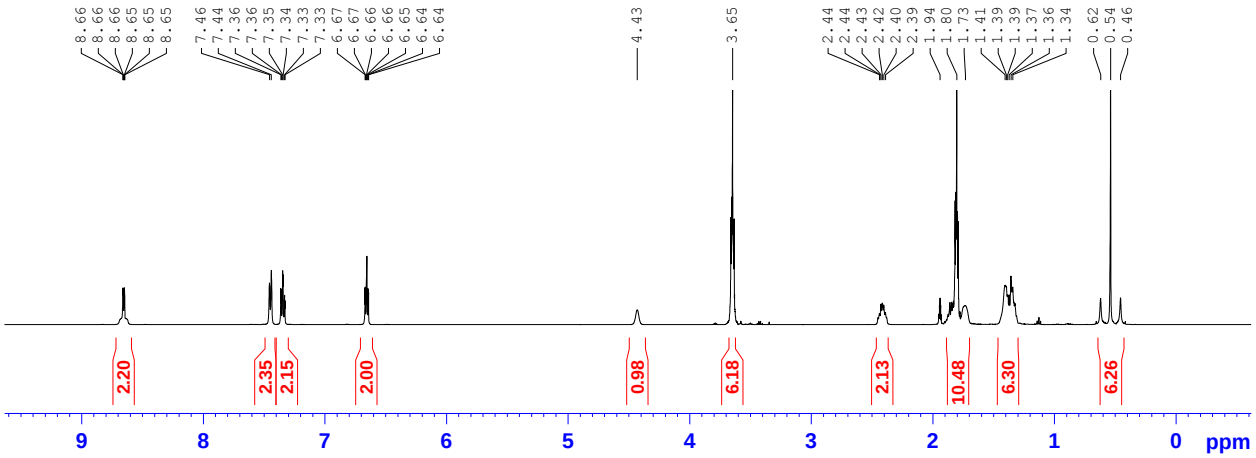

^{13}C NMR spectrum of Na[**2**]·1.5THF in CD_3CN (22°C, 125.769 MHz)

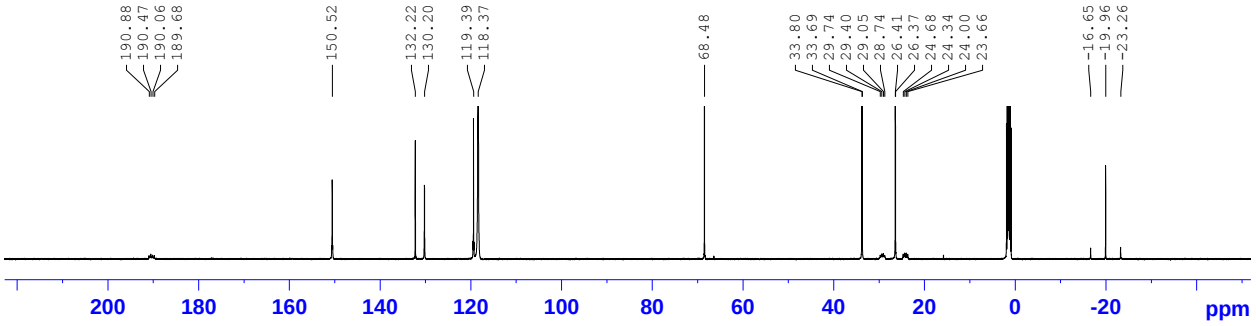

D4

Na[3]

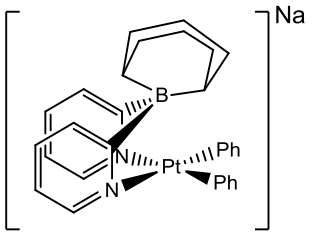

^{1}H NMR spectrum of Na[**3**]·1.4THF in CD_3CN (22°C, 500.132 MHz)

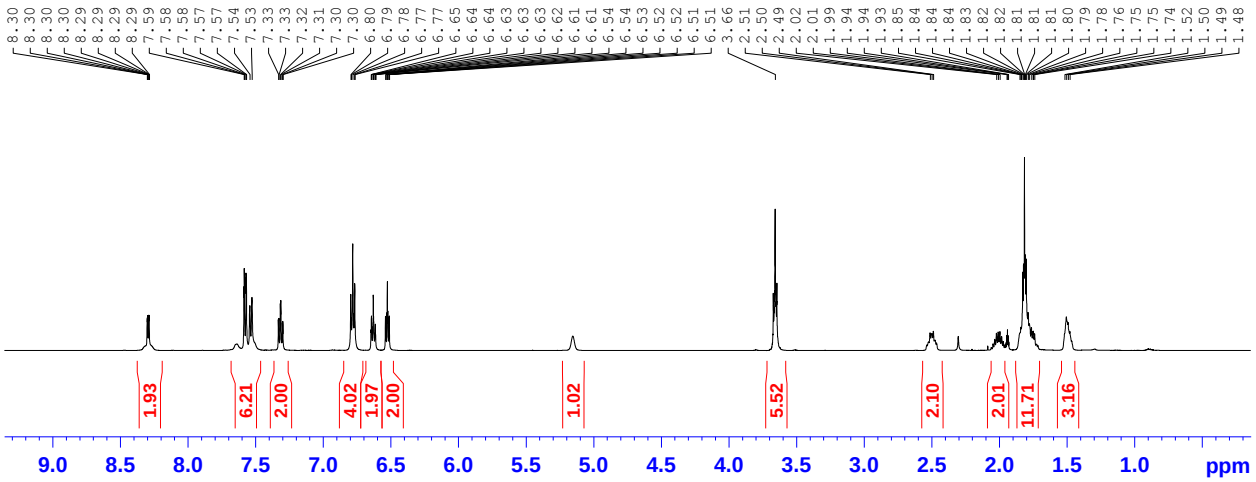

^{13}C NMR spectrum of Na[**3**]·1.4THF in CD_3CN (22°C, 125.769 MHz)

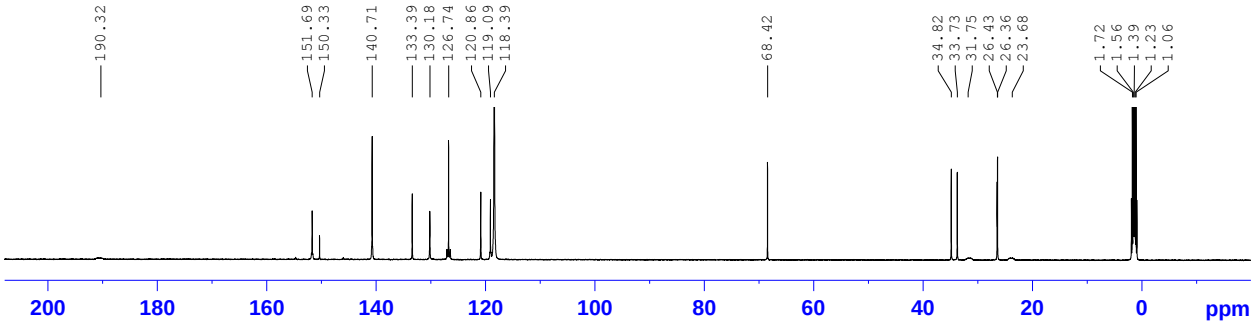

D5

Na[4]

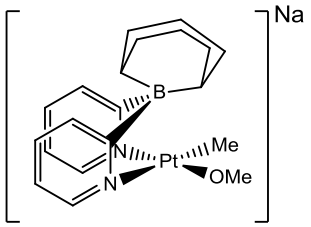

^{1}H NMR spectrum of Na[**4**] in THF-d_8 (22°C, 500.132 MHz)

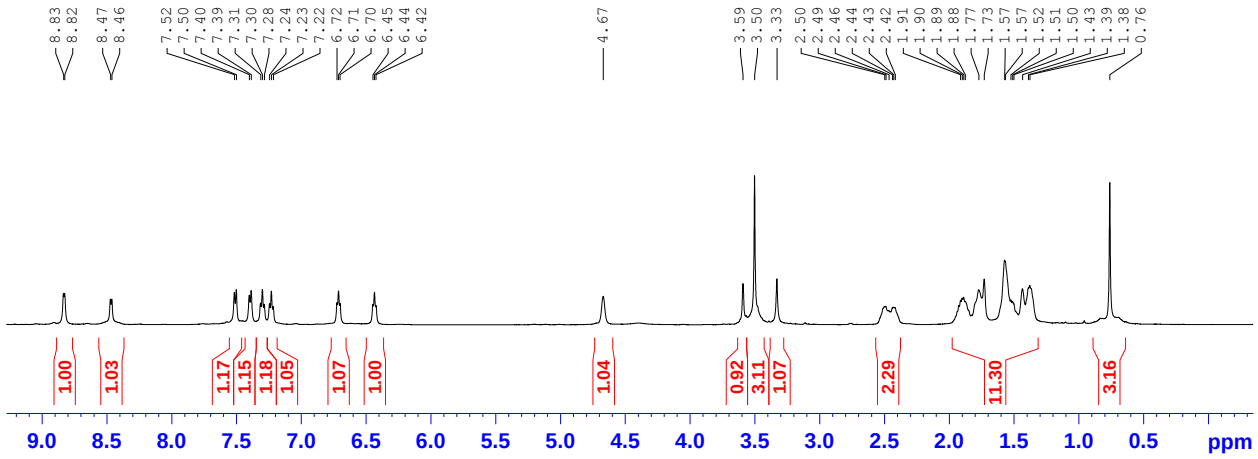

^{13}C NMR spectrum in THF-d_8 (22°C, 125.769 MHz); the signal at 50.0 ppm corresponds to traces MeOH.

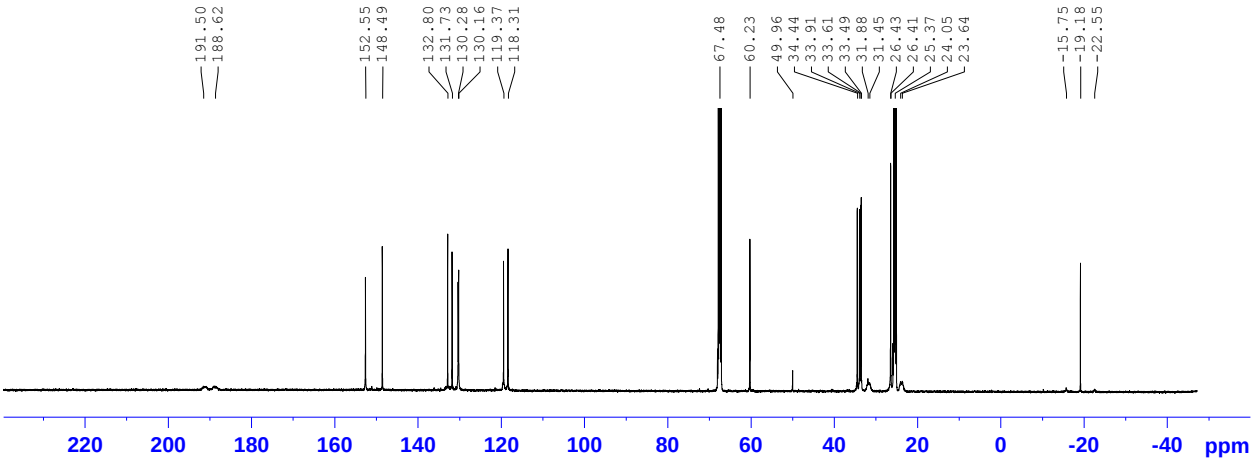

D6

^{13}C DEPT 45, 90, 135 NMR spectra of Na[**4**] in THF-d_8 (22°C, 125.769 MHz)

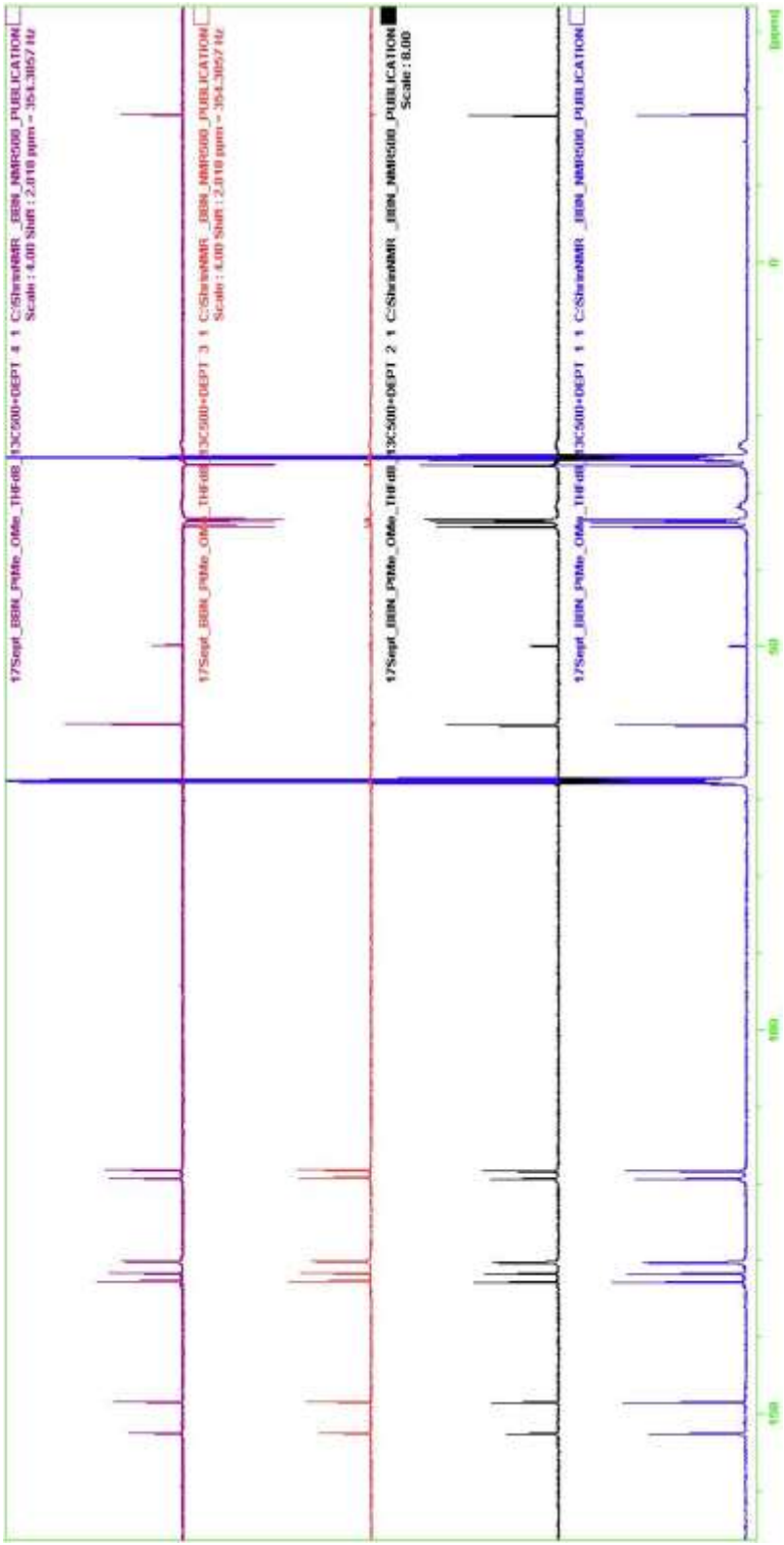

D7

Na[5]

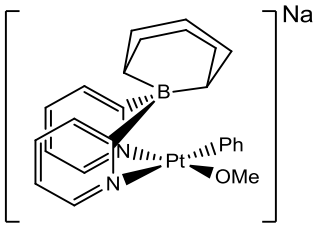

^{1}H NMR spectrum of Na[**5**]·1.0THF in THF-d_8 (22°C, 500.132 MHz)

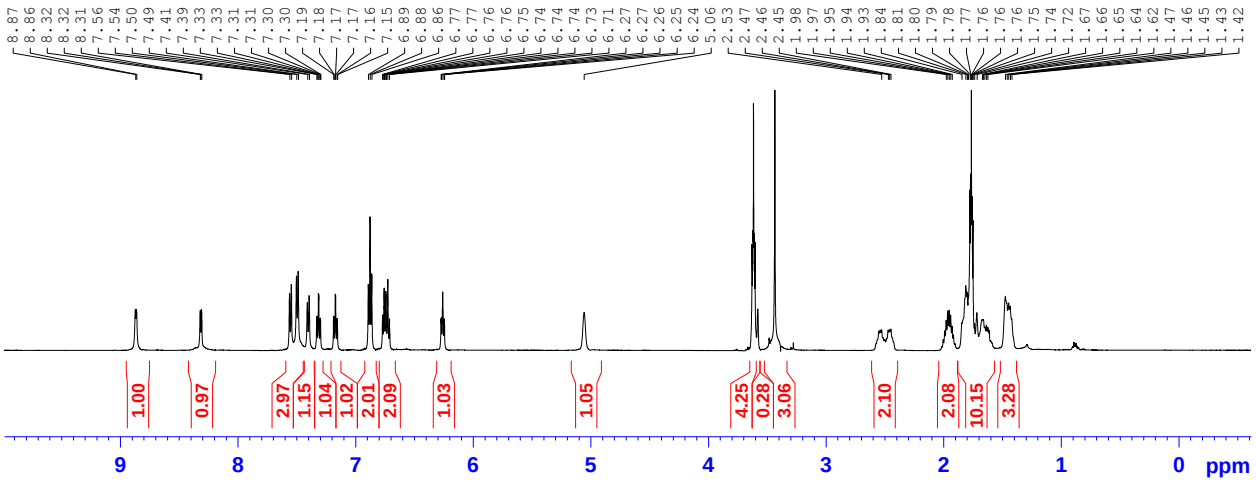

^{13}H NMR spectrum of Na[**5**]·1.0THF in THF-d_8 (22°C, 125.769 MHz)

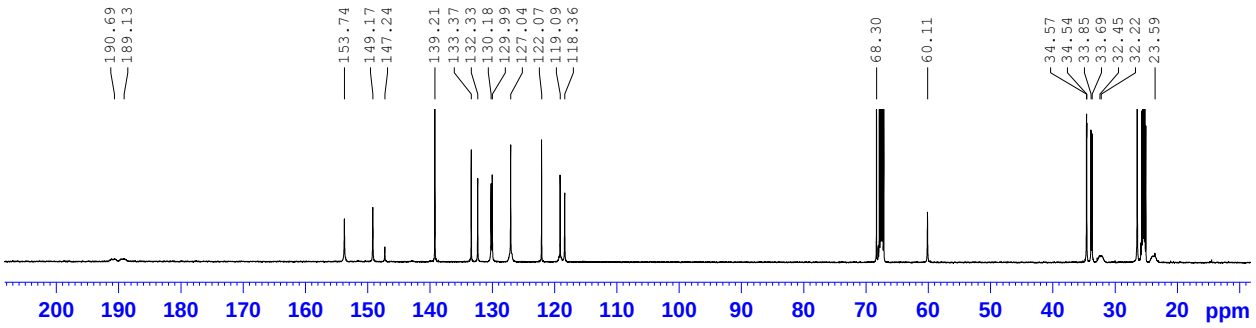

D8

Na[6]

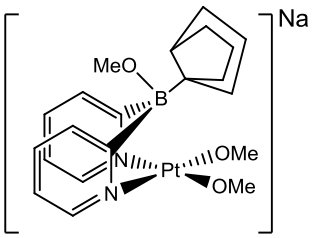

^{1}H NMR spectrum of Na[**6**]·0.4THF in CD_3CN (22°C, 400.131 MHz)

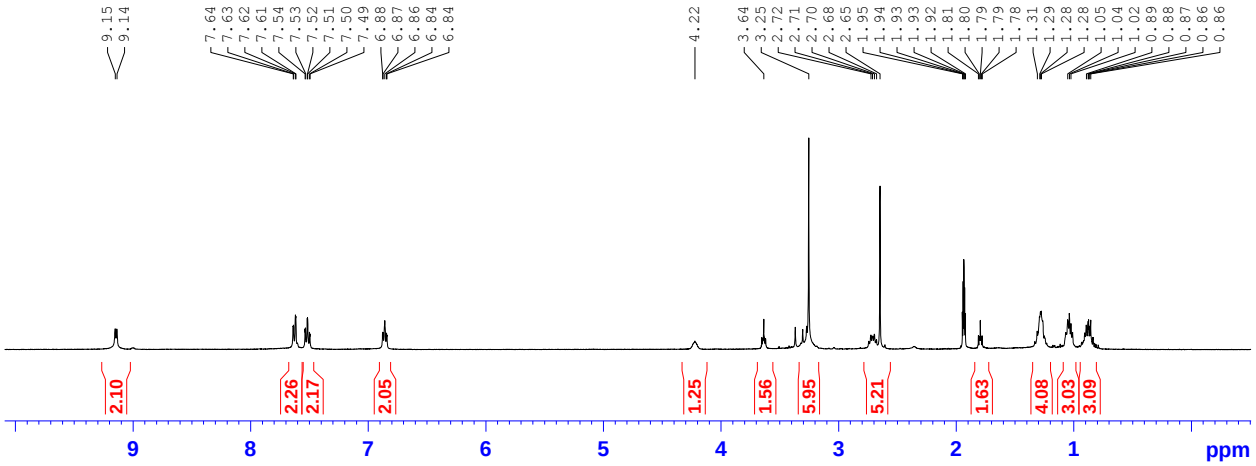

^{13}C NMR spectrum of Na[**6**] in DMSO-d_6 (22°C, 125.769 MHz)

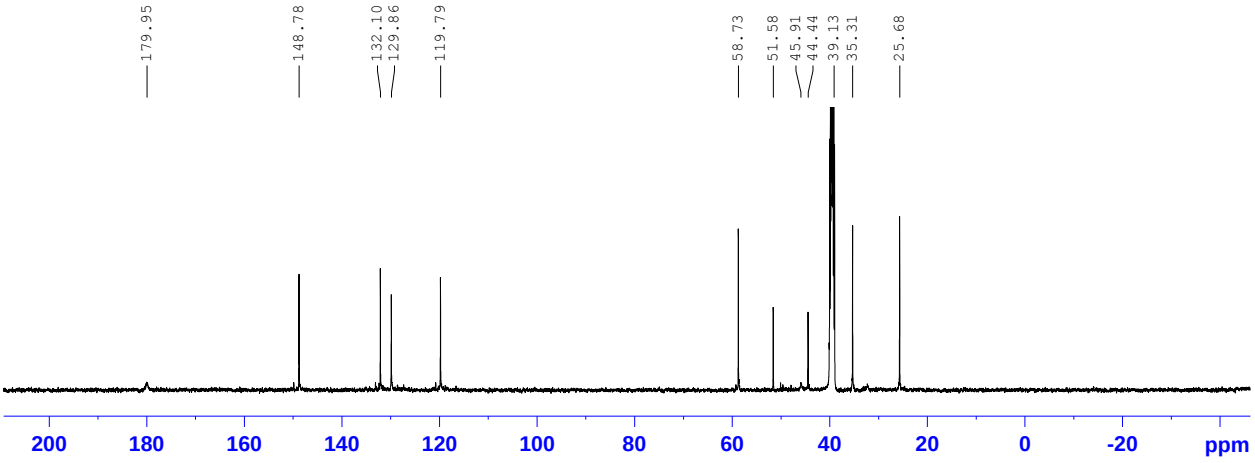

D9

10

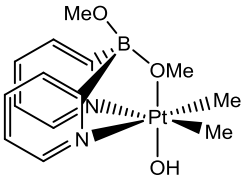

^{1}H NMR spectrum of **10** in $CDCl_3$(22°C, 400.131 MHz)

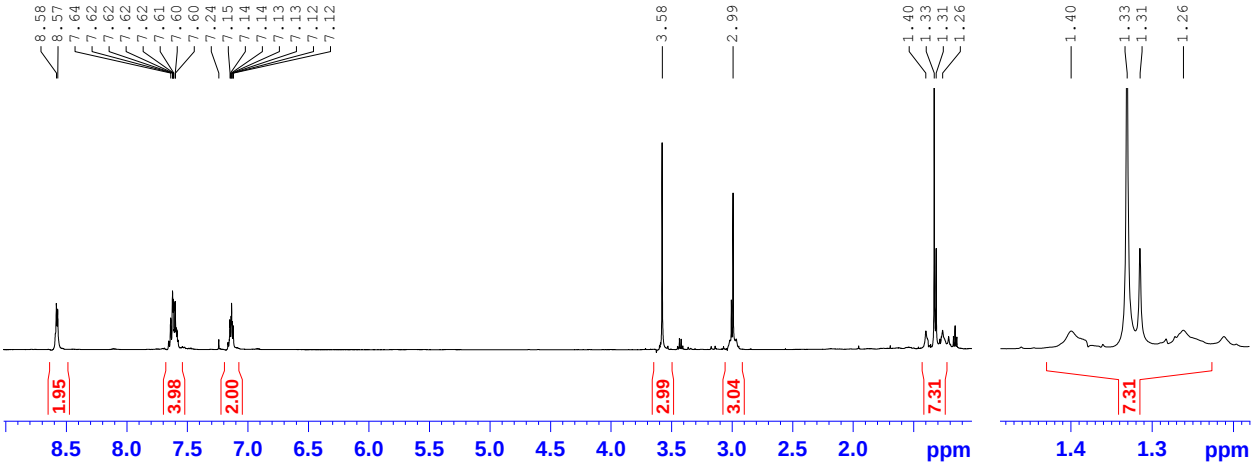

D10

11

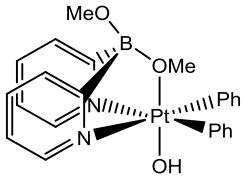

^{1}H NMR spectrum of **11·0.3THF** in $CDCl_3$(22°C, 500.132 MHz)

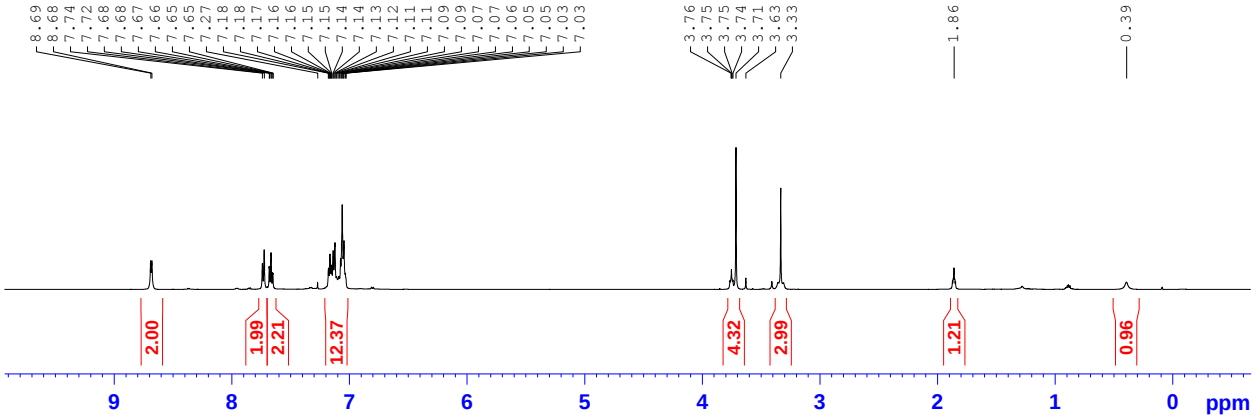

^{13}C NMR spectrum of **11** in $CDCl_3$ (22°C, 125.769 MHz)

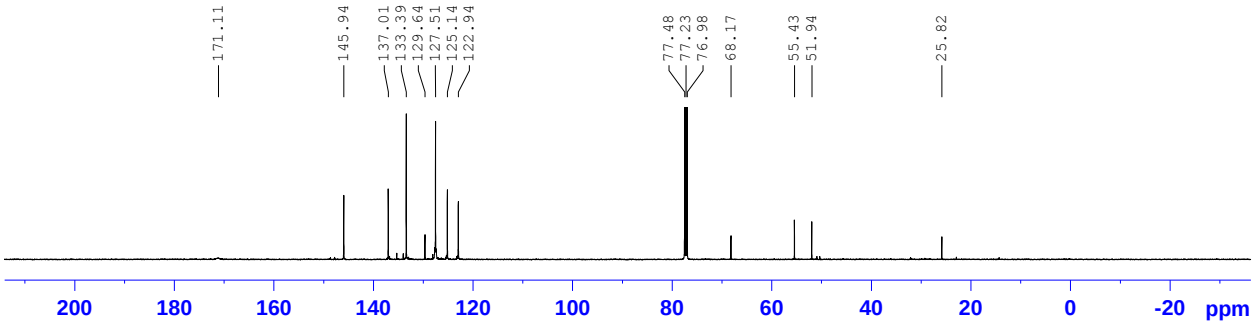

D11

9

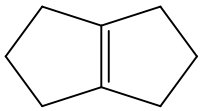

^{1}H NMR spectrum of **9** in *cyclo*-C_6D_{12} (22°C, 500.132 MHz)

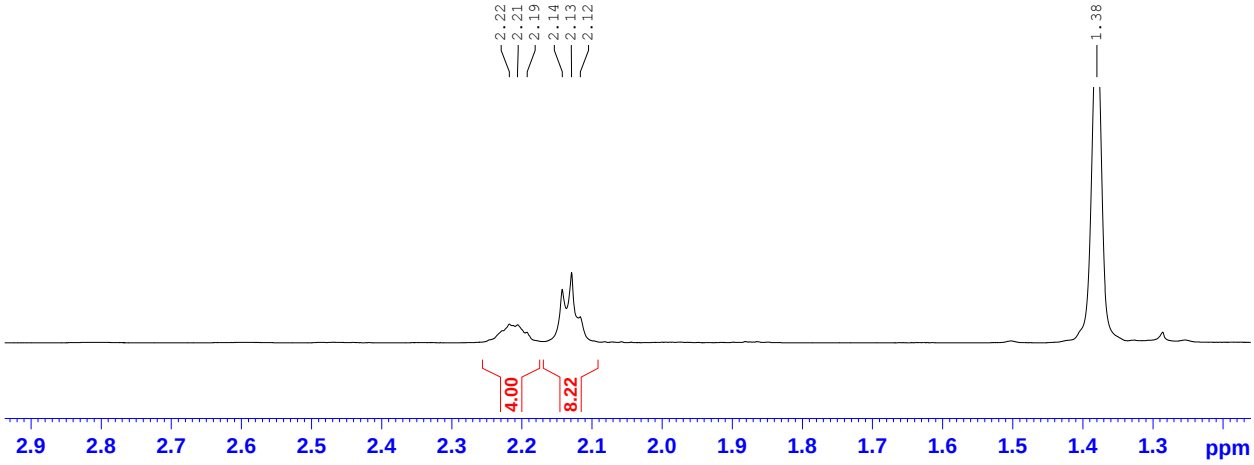

^{13}C NMR spectrum of **9** in *cyclo*-C_6D_{12} (22°C, 125.769 MHz)

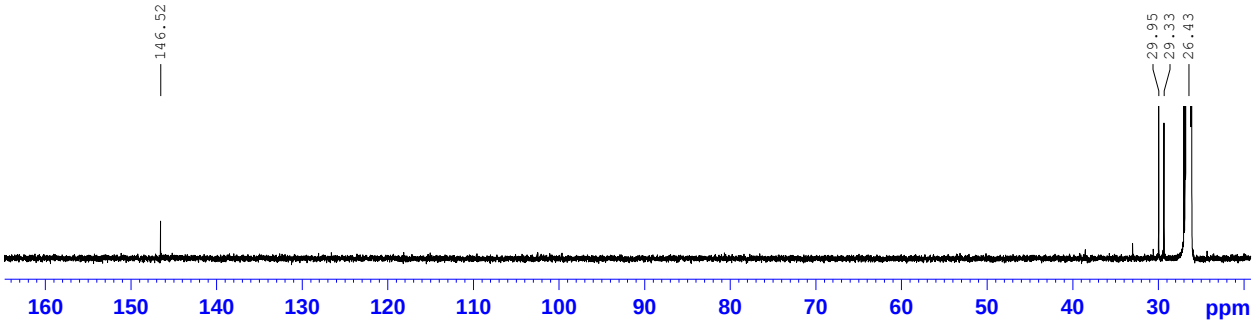

D12

13

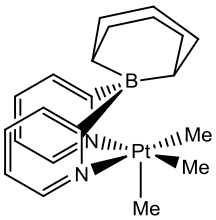

^{1}H NMR spectrum of **13** in CD_2Cl_2 (22°C, 500.132 MHz)

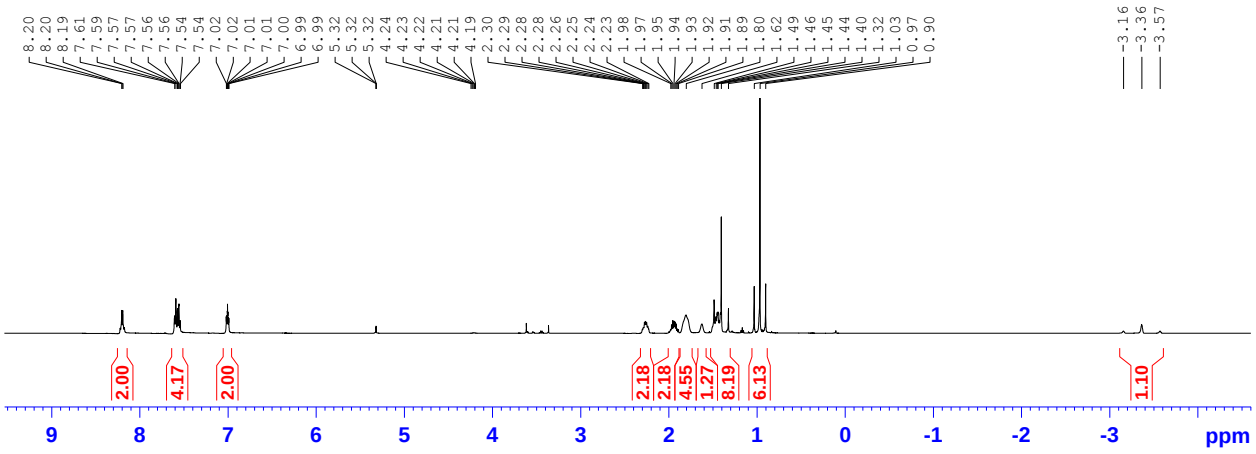

^{1}H NMR spectrum of **13** in CD_2Cl_2 (22°C, 125.769 MHz)

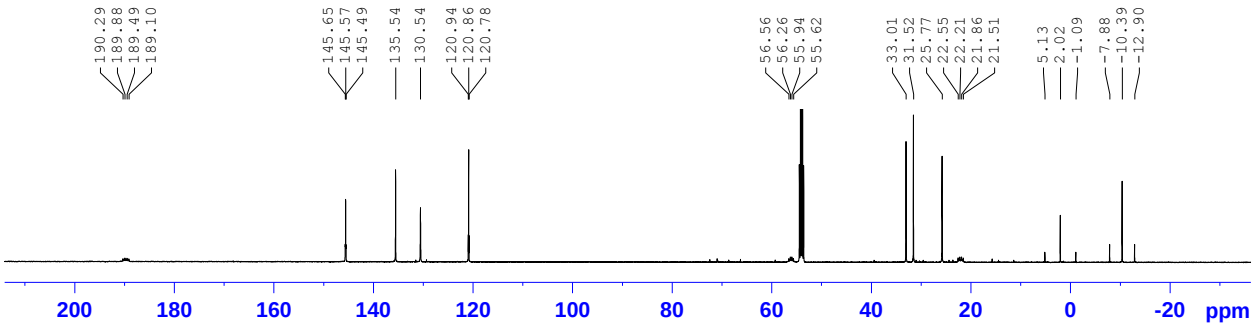

D13

Na[15]

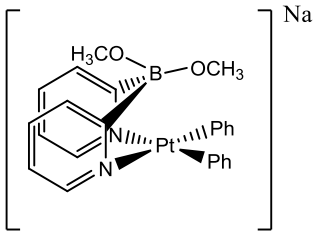

^{1}H NMR spectrum of Na[**15**] in CD_3OD (22°C, 400.131 MHz)

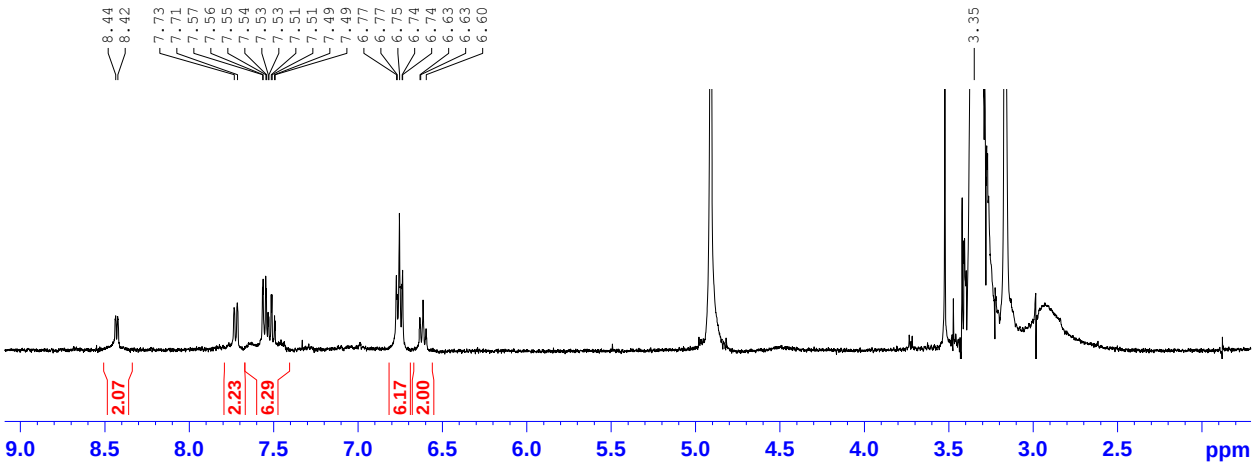

D14

Na[4-*d*$_6$]

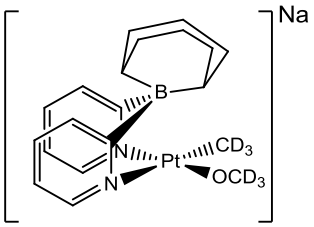

^{1}H NMR spectrum of Na[**4-*d*$_6$**] in CD_3OD (22°C, 500.132 MHz)

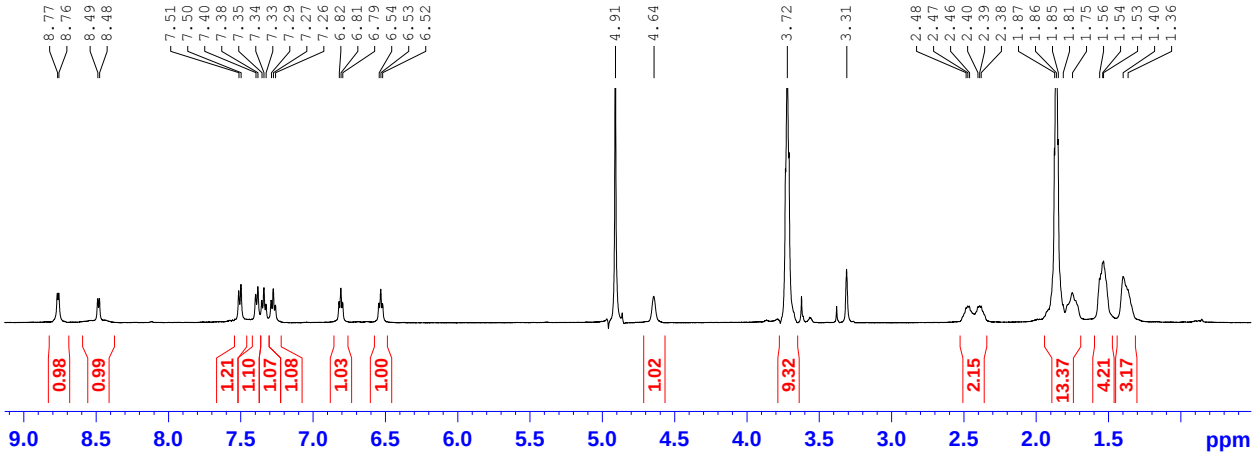

^{13}C NMR spectrum of Na[**4-*d*$_6$**] in CD_3OD (22°C, 125.769 MHz)

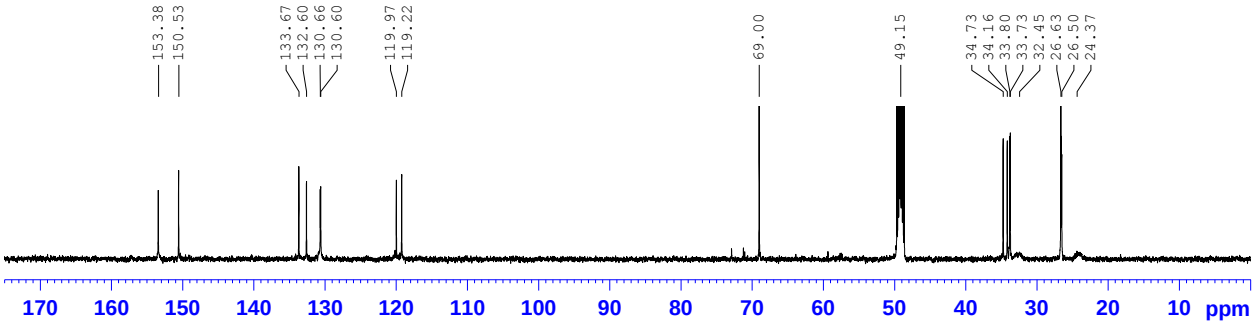

E. X-Ray crystal structure determinations of 1-H·HCl, Na[6], 11, 13

Crystal structure determination for 13

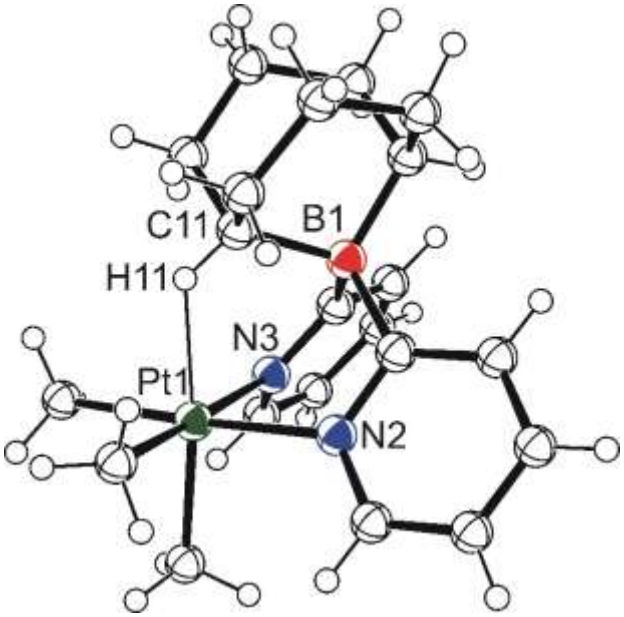

A colorless prism-like specimen of $C_{21}H_{31}BN_2Pt$, approximate dimensions 0.10 mm × 0.21 mm × 0.30 mm, was used for the X-ray crystallographic analysis. The X-ray intensity data were measured. Data collection temperature was 150 K.

The total exposure time was 10.10 hours. The frames were integrated with the Bruker SAINT software package using a narrow-frame algorithm. The integration of the data using a monoclinic unit cell yielded a total of 31911 reflections to a maximum θ angle of 29.99° (0.71 Å resolution), of which 5790 were independent (average redundancy 5.511, completeness = 99.9%, R_{int} = 2.64%, R_{sig} = 1.81%) and 5236 (90.43%) were greater than $2\sigma(F^2)$. The final cell constants of a = 13.7998(10) Å, b = 10.3648(8) Å, c = 14.9296(11) Å, β = 111.4900(10)°, V = 1987.0(3) $Å^3$, are based upon the refinement of the XYZ-centroids of 9850 reflections above 20 σ(I) with 5.050° < 2θ < 64.49°. The calculated minimum and maximum transmission coefficients (based on crystal size) are 0.2256 and 0.5384.
The structure was solved and refined using the Bruker SHELXTL Software Package, using the space group P 1 21/c 1, with Z = 4 for the formula unit, $C_{21}H_{31}BN_2Pt$. The final anisotropic full-matrix least-squares refinement on F^2 with 458 variables converged at R_1 = 2.51%, for the observed data and wR_2 = 5.50% for all data. The goodness-of-fit was 1.000. The largest peak in the final difference electron density synthesis was 3.467 $e^-/Å^3$ and the largest hole was -1.913 $e^-/Å^3$ with an RMS deviation of 0.108 $e^-/Å^3$. On the basis of the final model, the calculated density was 1.730 g/cm^3 and F(000), 1016 e^-
.

APEX2 Version 2010.11-3 (Bruker AXS Inc.)
SAINT Version 7.68A (Bruker AXS Inc., 2009)
SADABS Version 2008/1 (G. M. Sheldrick, Bruker AXS Inc.)

XPREP Version 2008/2 (G. M. Sheldrick, Bruker AXS Inc.)
XS Version 2008/1 (G. M. Sheldrick, *Acta Cryst.* (2008). A**64**, 112-122)
XL Version 2012 (G. M. Sheldrick, 2012)
Platon (A. L. Spek, *Acta Cryst.* (1990). A**46**, C-34)

Table 1. Sample and crystal data for UM2334.

Identification code	2334	
Chemical formula	$C_{21}H_{31}BN_2Pt$	
Formula weight	517.38	
Temperature	150(2) K	
Wavelength	0.71073 Å	
Crystal size	0.10 × 0.21 × 0.30 mm	
Crystal habit	colorless prism	
Crystal system	monoclinic	
Space group	P 1 21/c 1	
Unit cell dimensions	a = 13.7998(10) Å	α = 90°
	b = 10.3648(8) Å	β = 111.4900(10)°
	c = 14.9296(11) Å	γ = 90°
Volume	1987.0(3) $Å^3$	
Z	4	
Density (calculated)	1.730 Mg/cm^3	
Absorption coefficient	7.067 mm^{-1}	
F(000)	1016	

Table 2. Data collection and structure refinement for UM2334.

Theta range for data collection	2.45 to 29.99°	
Index ranges	$-19 \leq h \leq 19$, $-14 \leq k \leq 14$, $-20 \leq l \leq 21$	
Reflections collected	31911	
Independent reflections	5790 [R(int) = 0.0264]	
Coverage of independent reflections	99.9%	
Max. and min. transmission	0.5384 and 0.2256	
Structure solution technique	direct methods	
Structure solution program	SHELXS-97 (Sheldrick, 2008)	
Refinement method	Full-matrix least-squares on F^2	
Refinement program	SHELXL-2012 (Sheldrick, 2012)	
Function minimized	$\Sigma\, w(F_o^2 - F_c^2)^2$	
Data / restraints / parameters	5790 / 706 / 458	
Goodness-of-fit on F^2	1.000	
Δ/σ_{max}	0.001	
Final R indices	5236 data; $I>2\sigma(I)$	$R_1 = 0.0251$, $wR_2 = 0.0536$
	all data	$R_1 = 0.0296$, $wR_2 = 0.0550$
Weighting scheme	$w=1/[\sigma^2(F_o^2)+(0.0100P)^2+7.6500P]$, $P=(F_o^2+2F_c^2)/3$	
Largest diff. peak and hole	3.467 and -1.913 eÅ^{-3}	
R.M.S. deviation from mean	0.108 eÅ^{-3}	

$R_{int} = \Sigma|F_o^2 - F_o^2(\text{mean})| / \Sigma[F_o^2]$
$R_1 = \Sigma||F_o| - |F_c|| / \Sigma|F_o|$
$\text{GOOF} = S = \{\Sigma[w(F_o^2 - F_c^2)^2] / (n - p)\}^{1/2}$
$wR_2 = \{\Sigma[w(F_o^2 - F_c^2)^2] / \Sigma[w(F_o^2)^2]\}^{1/2}$

Table 3. Atomic coordinates and equivalent isotropic atomic displacement parameters (Å^2) for UM2334.

U(eq) is defined as one third of the trace of the orthogonalized U_{ij} tensor.

	x/a	y/b	z/c	U(eq)
Pt1	0.310504(10)	0.483822(10)	0.161229(8)	0.02655(4)
C1	0.3809(4)	0.3071(3)	0.1768(3)	0.0464(10)
C2	0.1985(4)	0.3990(4)	0.2053(4)	0.0512(11)
C3	0.4020(3)	0.5196(4)	0.3035(3)	0.0418(8)
B1	0.2542(3)	0.7035(3)	0.0173(2)	0.0235(6)
C11	0.2242(2)	0.7208(3)	0.1136(2)	0.0264(6)
C12	0.2852(3)	0.8351(3)	0.1745(3)	0.0318(7)
C13	0.2667(3)	0.9641(3)	0.1202(3)	0.0409(9)
C14	0.2693(3)	0.9556(3)	0.0191(3)	0.0421(9)
C15	0.2124(3)	0.8380(3)	0.9584(3)	0.0350(7)
C16	0.0929(3)	0.8494(4)	0.9306(3)	0.0494(10)
C17	0.0534(3)	0.8356(4)	0.0135(4)	0.0503(11)
C18	0.1053(3)	0.7277(4)	0.0858(3)	0.0393(8)
N2	0.41896(19)	0.5786(2)	0.11238(17)	0.0216(5)
C21	0.3787(2)	0.6759(3)	0.0477(2)	0.0217(5)
C22	0.4464(3)	0.7389(3)	0.0110(2)	0.0309(7)
C23	0.5511(3)	0.7055(4)	0.0419(3)	0.0368(8)
C24	0.5885(3)	0.6065(4)	0.1064(3)	0.0373(8)
C25	0.5203(3)	0.5452(3)	0.1404(2)	0.0311(7)
N3	0.2166(2)	0.4616(3)	0.0115(2)	0.0272(5)
C31	0.2026(2)	0.5721(3)	0.9585(2)	0.0261(6)
C32	0.1514(3)	0.5619(4)	0.8583(3)	0.0373(7)
C33	0.1155(3)	0.4425(5)	0.8155(3)	0.0464(10)
C34	0.1294(4)	0.3345(4)	0.8717(3)	0.0443(10)
C35	0.1804(4)	0.3470(4)	0.9696(3)	0.0372(8)
Pt1A	0.21339(19)	0.7841(2)	0.01588(19)	0.0344(9)
C1A	0.202(3)	0.883(3)	0.8932(17)	0.047(7)
C2A	0.0609(13)	0.841(3)	0.991(4)	0.048(6)
C3A	0.268(3)	0.954(2)	0.090(3)	0.037(7)
B1A	0.2996(16)	0.5192(18)	0.1009(15)	0.028(3)
C11A	0.253(2)	0.612(2)	0.1655(19)	0.031(3)
C12A	0.340(3)	0.648(4)	0.262(2)	0.037(5)
C13A	0.437(3)	0.562(4)	0.293(3)	0.041(5)
C14A	0.420(3)	0.420(3)	0.265(2)	0.039(5)

	x/a	y/b	z/c	U(eq)
C15A	0.335(2)	0.388(2)	0.1664(19)	0.038(4)
C16A	0.237(3)	0.327(3)	0.178(3)	0.039(4)
C17A	0.170(4)	0.415(4)	0.213(5)	0.038(5)
C18A	0.155(2)	0.553(3)	0.174(3)	0.034(4)
N2A	0.3677(11)	0.718(2)	0.043(3)	0.027(3)
C21A	0.3913(16)	0.596(2)	0.078(3)	0.025(3)
C22A	0.4957(19)	0.556(4)	0.105(4)	0.030(3)
C23A	0.564(2)	0.624(4)	0.073(5)	0.032(3)
C24A	0.531(3)	0.737(5)	0.023(5)	0.032(3)
C25A	0.438(2)	0.789(3)	0.021(4)	0.028(3)
N3A	0.164(2)	0.6028(12)	0.9437(16)	0.032(3)
C31A	0.212(3)	0.4960(14)	0.9934(18)	0.031(3)
C32A	0.177(6)	0.3757(18)	0.950(3)	0.037(3)
C33A	0.121(8)	0.369(3)	0.850(3)	0.041(3)
C34A	0.100(6)	0.482(4)	0.798(2)	0.042(3)
C35A	0.105(4)	0.595(3)	0.8488(19)	0.041(3)

Table 4. Bond lengths (Å) for UM2334.

Pt1-C1	2.046(3)	Pt1-C3	2.068(4)
Pt1-C2	2.083(4)	Pt1-N2	2.130(3)
Pt1-N3	2.147(3)	Pt1-H11	1.99(4)
C1-H1A	0.98	C1-H1B	0.98
C1-H1C	0.98	C2-H2A	0.98
C2-H2B	0.98	C2-H2C	0.98
C3-H3A	0.98	C3-H3B	0.98
C3-H3C	0.98	B1-C21	1.633(4)
B1-C31	1.636(4)	B1-C15	1.637(5)
B1-C11	1.646(5)	C11-C18	1.540(4)
C11-C12	1.541(4)	C11-H11	0.96(4)
C12-C13	1.536(5)	C12-H12A	0.99
C12-H12B	0.99	C13-C14	1.526(6)
C13-H13A	0.99	C13-H13B	0.99
C14-C15	1.550(5)	C14-H14A	0.99
C14-H14B	0.99	C15-C16	1.550(5)
C15-H15	1.0	C16-C17	1.531(7)
C16-H16A	0.99	C16-H16B	0.99
C17-C18	1.537(6)	C17-H17A	0.99
C17-H17B	0.99	C18-H18A	0.99
C18-H18B	0.99	N2-C25	1.350(4)
N2-C21	1.365(4)	C21-C22	1.405(4)
C22-C23	1.390(5)	C22-H22	0.95
C23-C24	1.372(6)	C23-H23	0.95
C24-C25	1.377(5)	C24-H24	0.95
C25-H25	0.95	N3-C35	1.350(4)
N3-C31	1.364(4)	C31-C32	1.404(5)
C32-C33	1.398(6)	C32-H32	0.95
C33-C34	1.369(7)	C33-H33	0.95
C34-C35	1.377(6)	C34-H34	0.95
C35-H35	0.95		

Crystal structure determination for 11

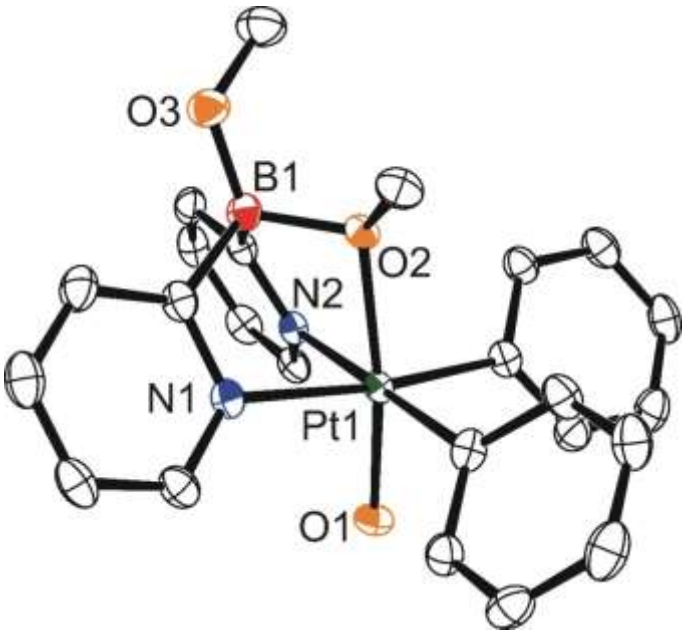

A colorless plate-like specimen of $C_{28}H_{33}BN_2O_4Pt$, approximate dimensions 0.01 mm × 0.14 mm × 0.17 mm, was used for the X-ray crystallographic analysis. The X-ray intensity data were measured. Data collection temperature was 150 K.

The total exposure time was 22.72 hours. The frames were integrated with the Bruker SAINT software package using a narrow-frame algorithm. The integration of the data using a triclinic unit cell yielded a total of 15028 reflections to a maximum θ angle of 30.00° (0.71 Å resolution), of which 7376 were independent (average redundancy 2.037, completeness = 99.0%, R_{int} = 2.76%) and 6508 (88.23%) were greater than $2\sigma(F^2)$. The final cell constants of a = 8.7630(7) Å, b = 12.1564(9) Å, c = 13.1947(10) Å, α = 107.2164(10)°, β = 103.3376(10)°, γ = 97.3974(11)°, V = 1276.70(17) $Å^3$, are based upon the refinement of the XYZ-centroids of 7006 reflections above 20 σ(I) with 4.888° < 2θ < 61.80°. The final anisotropic full-matrix least-squares refinement on F^2 with 355 variables converged at R_1 = 2.65%, for the observed data and wR_2 = 5.80% for all data. The goodness-of-fit was 1.000. The largest peak in the final difference electron density synthesis was 1.067 $e^-/Å^3$ and the largest hole was -1.129 $e^-/Å^3$ with an RMS deviation of 0.132 $e^-/Å^3$. On the basis of the final model, the calculated density was 1.736 g/cm^3 and F(000), 660 e^-.

APEX2 Version 2010.11-3 (Bruker AXS Inc.)
SAINT Version 7.68A (Bruker AXS Inc., 2009)
SADABS Version 2008/1 (G. M. Sheldrick, Bruker AXS Inc.)
XPREP Version 2008/2 (G. M. Sheldrick, Bruker AXS Inc.)
XS Version 2008/1 (G. M. Sheldrick, *Acta Cryst.* (2008). A**64**, 112-122)
XL Version 2012/4 (G. M. Sheldrick, (2012) University of Gottingen, Germany)
Platon (A. L. Spek, *Acta Cryst.* (1990). A**46**, C-34)

Table 1. Sample and crystal data for UM2364.

Identification code	2364	
Chemical formula	$C_{28}H_{33}BN_2O_4Pt$	
Formula weight	667.46	
Temperature	150(2) K	
Wavelength	0.71073 Å	
Crystal size	0.01 × 0.14 × 0.17 mm	
Crystal habit	colorless plate	
Crystal system	triclinic	
Unit cell dimensions	a = 8.7630(7) Å	α = 107.2164(10)°
	b = 12.1564(9) Å	β = 103.3376(10)°
	c = 13.1947(10) Å	γ = 97.3974(11)°
Volume	1276.70(17) $Å^3$	
Z	2	
Density (calculated)	1.736 Mg/cm^3	
Absorption coefficient	5.533 mm^{-1}	
F(000)	660	

Table 2. Data collection and structure refinement for UM2364.

Theta range for data collection	2.44 to 30.00°	
Index ranges	$-12 \leq h \leq 12$, $-17 \leq k \leq 17$, $-18 \leq l \leq 18$	
Reflections collected	15028	
Independent reflections	7376 [R(int) = 0.0276]	
Coverage of independent reflections	99.0%	
Refinement method	Full-matrix least-squares on F^2	
Refinement program	SHELXL-2012 (Sheldrick, 2012)	
Function minimized	$\Sigma\, w(F_o^2 - F_c^2)^2$	
Data / restraints / parameters	7376 / 1 / 355	
Goodness-of-fit on F^2	1.000	
Δ/σ_{max}	0.002	
Final R indices	6508 data; $I>2\sigma(I)$	$R_1 = 0.0265$, $wR_2 = 0.0551$
	all data	$R_1 = 0.0349$, $wR_2 = 0.0580$
Weighting scheme	$w=1/[\sigma^2(F_o^2)+(0.0240P)^2+0.9050P]$, $P=(F_o^2+2F_c^2)/3$	
Largest diff. peak and hole	1.067 and -1.129 eÅ^{-3}	
R.M.S. deviation from mean	0.132 eÅ^{-3}	

$R_{int} = \Sigma|F_o^2 - F_o^2(\text{mean})| / \Sigma[F_o^2]$
$R_1 = \Sigma||F_o| - |F_c|| / \Sigma|F_o|$
$\text{GOOF} = S = \{\Sigma[w(F_o^2 - F_c^2)^2] / (n - p)\}^{1/2}$
$wR_2 = \{\Sigma[w(F_o^2 - F_c^2)^2] / \Sigma[w(F_o^2)^2]\}^{1/2}$

Table 3. Atomic coordinates and equivalent isotropic atomic displacement parameters (Å^2) for UM2364.

U(eq) is defined as one third of the trace of the orthogonalized U_{ij} tensor.

	x/a	y/b	z/c	U(eq)
Pt1	0.57237(2)	0.06502(2)	0.24727(2)	0.01677(4)
O1	0.5836(3)	0.9829(2)	0.09665(18)	0.0248(5)
B1	0.6823(4)	0.2959(3)	0.4095(3)	0.0221(7)
O2	0.6022(3)	0.17351(19)	0.40954(17)	0.0194(4)
C2	0.4729(4)	0.1764(3)	0.4600(3)	0.0277(7)
O3	0.7099(3)	0.3892(2)	0.51211(19)	0.0289(5)
C3	0.8091(5)	0.3779(4)	0.6088(3)	0.0370(9)
N1	0.4983(3)	0.2206(2)	0.2171(2)	0.0201(5)
C11	0.5593(4)	0.3183(3)	0.3091(3)	0.0218(6)
C12	0.5155(4)	0.4243(3)	0.3087(3)	0.0281(7)
C13	0.4124(4)	0.4308(3)	0.2144(3)	0.0327(8)
C14	0.3559(4)	0.3313(3)	0.1210(3)	0.0298(8)
C15	0.4014(4)	0.2274(3)	0.1251(3)	0.0253(7)
N2	0.8087(3)	0.1627(2)	0.2876(2)	0.0190(5)
C21	0.8400(4)	0.2666(3)	0.3698(3)	0.0215(6)
C22	0.9937(4)	0.3369(3)	0.4050(3)	0.0245(7)
C23	0.1117(4)	0.3012(3)	0.3571(3)	0.0276(7)
C24	0.0750(4)	0.1935(3)	0.2721(3)	0.0276(7)
C25	0.9206(4)	0.1254(3)	0.2389(3)	0.0225(6)
C31	0.3427(4)	0.9721(3)	0.2080(3)	0.0218(6)
C32	0.2333(4)	0.9536(3)	0.1061(3)	0.0244(7)
C33	0.0760(4)	0.8922(3)	0.0791(3)	0.0289(7)
C34	0.0229(4)	0.8480(3)	0.1533(3)	0.0334(8)
C35	0.1305(4)	0.8633(3)	0.2537(3)	0.0324(8)
C36	0.2881(4)	0.9230(3)	0.2801(3)	0.0269(7)
C41	0.6555(4)	0.9346(3)	0.2943(3)	0.0206(6)
C42	0.7613(4)	0.9614(3)	0.3993(3)	0.0245(7)
C43	0.8208(4)	0.8730(3)	0.4331(3)	0.0283(7)
C44	0.7775(4)	0.7581(3)	0.3633(3)	0.0313(8)
C45	0.6741(5)	0.7308(3)	0.2585(3)	0.0330(8)
C46	0.6133(4)	0.8184(3)	0.2245(3)	0.0285(7)
O5	0.7920(4)	0.5261(3)	0.0390(3)	0.0528(8)
C51	0.6911(6)	0.4124(4)	0.9973(4)	0.0522(12)
C52	0.7547(5)	0.3484(4)	0.0747(4)	0.0515(12)

	x/a	y/b	z/c	U(eq)
C53	0.9292(6)	0.4033(4)	0.1159(4)	0.0476(11)
C54	0.9282(5)	0.5301(4)	0.1248(4)	0.0424(10)

Table 4. Bond lengths (Å) for UM2364.

Pt1-O1	1.974(2)	Pt1-C41	2.026(3)
Pt1-C31	2.045(3)	Pt1-O2	2.091(2)
Pt1-N2	2.113(3)	Pt1-N1	2.191(3)
O1-H1	0.795(10)	B1-O3	1.430(4)
B1-O2	1.562(4)	B1-C11	1.619(5)
B1-C21	1.632(5)	O2-C2	1.440(4)
C2-H2A	0.98	C2-H2B	0.98
C2-H2C	0.98	O3-C3	1.423(4)
C3-H3A	0.98	C3-H3B	0.98
C3-H3C	0.98	N1-C15	1.343(4)
N1-C11	1.362(4)	C11-C12	1.392(4)
C12-C13	1.389(5)	C12-H12	0.95
C13-C14	1.381(5)	C13-H13	0.95
C14-C15	1.385(5)	C14-H14	0.95
C15-H15	0.95	N2-C21	1.345(4)
N2-C25	1.346(4)	C21-C22	1.393(4)
C22-C23	1.383(5)	C22-H22	0.95
C23-C24	1.389(5)	C23-H23	0.95
C24-C25	1.390(5)	C24-H24	0.95
C25-H25	0.95	C31-C32	1.396(5)
C31-C36	1.401(4)	C32-C33	1.391(5)
C32-H32	0.95	C33-C34	1.386(5)
C33-H33	0.95	C34-C35	1.382(5)
C34-H34	0.95	C35-C36	1.388(5)
C35-H35	0.95	C36-H36	0.95
C41-C46	1.384(5)	C41-C42	1.396(4)
C42-C43	1.396(5)	C42-H42	0.95
C43-C44	1.372(5)	C43-H43	0.95
C44-C45	1.384(5)	C44-H44	0.95
C45-C46	1.392(5)	C45-H45	0.95
C46-H46	0.95	O5-C51	1.416(5)
O5-C54	1.427(5)	C51-C52	1.510(7)

C51-H51A	0.99	C51-H51B	0.99
C52-C53	1.489(6)	C52-H52A	0.99
C52-H52B	0.99	C53-C54	1.512(6)
C53-H53A	0.99	C53-H53B	0.99
C54-H54A	0.99	C54-H54B	0.99

Crystal structure determination for Na[6]

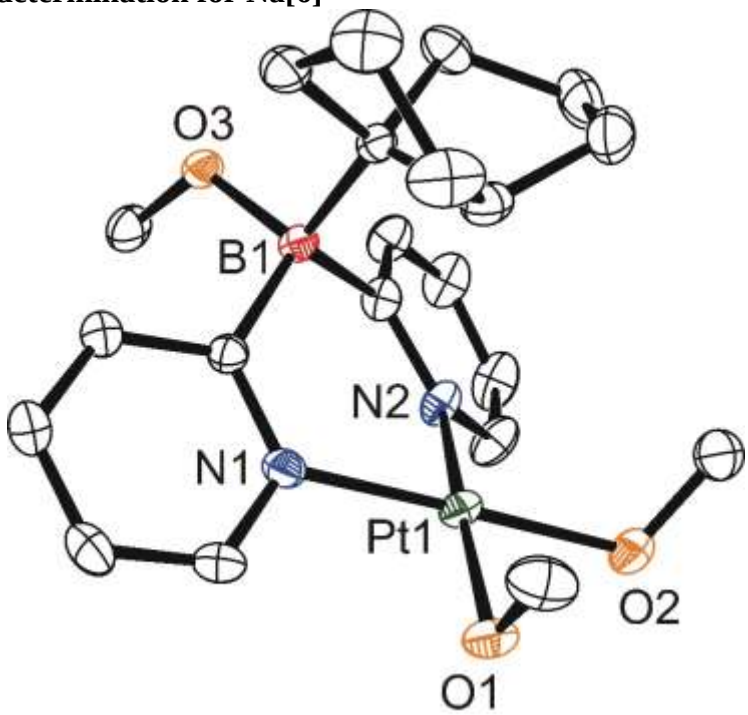

A colorless prism-like specimen of $C_{23}H_{36}BN_2NaO_{4.25}Pt$, approximate dimensions 0.12 mm × 0.16 mm × 0.19 mm, was used for the X-ray crystallographic analysis. The X-ray intensity data were measured on a Bruker APEX-II CCD system equipped with a graphite monochromator and a MoKα sealed tube (λ = 0.71073 Å). Data collection temperature was 150 K.

The total exposure time was 20.33 hours. The frames were integrated with the Bruker SAINT software package using a narrow-frame algorithm. The integration of the data using a monoclinic unit cell yielded a total of 60095 reflections to a maximum θ angle of 30.00° (0.71 Å resolution), of which 14457 were independent (average redundancy 4.157, completeness = 99.7%, R_{int} = 3.45%) and 12135 (83.94%) were greater than $2\sigma(F^2)$. The final cell constants of a = 17.5793(11) Å, b = 17.8585(11) Å, c = 17.6641(11) Å, β = 116.3130(8)°, V = 4970.9(5) $Å^3$, are based upon the refinement of the XYZ-centroids of 9851 reflections above 20 σ(I) with 4.561° < 2θ < 60.38°. Data were corrected for absorption effects using the multi-scan method (SADABS). The calculated minimum and maximum transmission coefficients (based on crystal size) are 0.4120 and 0.5050.
The structure was solved and refined using the Bruker SHELXTL Software Package, using the space group $P2_1/c$, with Z = 8 for the formula unit, $C_{23}H_{36}BN_2NaO_{4.25}Pt$. The final anisotropic full-matrix least-squares refinement on F^2 with 615 variables converged at R_1 = 3.14%, for the observed data and wR_2 = 6.97% for all data. The goodness-of-fit was 1.000. The largest peak in the final difference electron density synthesis was 3.259 $e^-/Å^3$ and the largest hole was -1.654 $e^-/Å^3$ with an RMS deviation of 0.123 $e^-/Å^3$. On the basis of the final model, the calculated density was 1.703 g/cm^3 and F(000), 2528 e^-.

APEX2 Version 2010.11-3 (Bruker AXS Inc.)
SAINT Version 7.68A (Bruker AXS Inc., 2009)
SADABS Version 2008/1 (G. M. Sheldrick, Bruker AXS Inc.)

XPREP Version 2008/2 (G. M. Sheldrick, Bruker AXS Inc.)
XS Version 2008/1 (G. M. Sheldrick, *Acta Cryst.* (2008). A**64**, 112-122)
XL Version 2012/4 (G. M. Sheldrick, (2012) University of Gottingen, Germany)
Platon (A. L. Spek, *Acta Cryst.* (1990). A**46**, C-34)

Table 1. Sample and crystal data for UM2369.

Identification code	2369	
Chemical formula	$C_{23}H_{36}BN_2NaO_{4.25}Pt$	
Formula weight	637.43	
Temperature	150(2) K	
Wavelength	0.71073 Å	
Crystal size	0.12 × 0.16 × 0.19 mm	
Crystal habit	colorless prism	
Crystal system	monoclinic	
Space group	$P2_1/c$	
Unit cell dimensions	a = 17.5793(11) Å	α = 90°
	b = 17.8585(11) Å	β = 116.3130(8)°
	c = 17.6641(11) Å	γ = 90°
Volume	4970.9(5) $Å^3$	
Z	8	
Density (calculated)	1.703 Mg/cm^3	
Absorption coefficient	5.695 mm^{-1}	
F(000)	2528	

Table 2. Data collection and structure refinement for UM2369.

Diffractometer	Bruker APEX-II CCD	
Radiation source	sealed tube, MoKα	
Theta range for data collection	2.28 to 30.00°	
Index ranges	$-24 \leq h \leq 24$, $-25 \leq k \leq 25$, $-24 \leq l \leq 24$	
Reflections collected	60095	
Independent reflections	14457 [R(int) = 0.0345]	
Coverage of independent reflections	99.7%	
Absorption correction	multi-scan	
Max. and min. transmission	0.5050 and 0.4120	
Structure solution technique	direct methods	
Structure solution program	ShelXS-97 (Sheldrick, 2008)	
Refinement method	Full-matrix least-squares on F^2	
Refinement program	ShelXL-2012 (Sheldrick, 2012)	
Function minimized	$\Sigma\, w(F_o^2 - F_c^2)^2$	
Data / restraints / parameters	14457 / 46 / 615	
Goodness-of-fit on F^2	1.000	
Δ/σ_{max}	0.002	
Final R indices	12135 data; I>2σ(I)	R_1 = 0.0314, wR_2 = 0.0657
	all data	R_1 = 0.0424, wR_2 = 0.0697
Weighting scheme	$w=1/[\sigma^2(F_o^2)+(0.0280P)^2+11.9000P]$, $P=(F_o^2+2F_c^2)/3$	
Largest diff. peak and hole	3.259 and -1.654 eÅ^{-3}	
R.M.S. deviation from mean	0.123 eÅ^{-3}	

$R_{int} = \Sigma|F_o^2 - F_o^2(\text{mean})| / \Sigma[F_o^2]$
$R_1 = \Sigma||F_o| - |F_c|| / \Sigma|F_o|$
$\text{GOOF} = S = \{\Sigma[w(F_o^2 - F_c^2)^2] / (n - p)\}^{1/2}$
$wR_2 = \{\Sigma[w(F_o^2 - F_c^2)^2] / \Sigma[w(F_o^2)^2]\}^{1/2}$

Table 3. Atomic coordinates and equivalent isotropic atomic displacement parameters (Å^2) for UM2369.

U(eq) is defined as one third of the trace of the orthogonalized U_{ij} tensor.

	x/a	y/b	z/c	U(eq)
Na1	0.29279(9)	0.53575(8)	0.29122(9)	0.0245(3)
Pt1	0.11715(2)	0.45602(2)	0.29237(2)	0.02033(3)
O1A	0.24454(15)	0.44466(14)	0.35017(16)	0.0264(5)
C1A	0.2761(2)	0.4114(3)	0.4301(3)	0.0360(9)
O2A	0.13538(16)	0.55990(13)	0.34261(17)	0.0274(5)
C2A	0.1112(3)	0.5667(2)	0.4092(3)	0.0328(8)
N1A	0.10370(17)	0.35123(16)	0.24512(17)	0.0212(6)
C11A	0.0341(2)	0.30715(18)	0.2282(2)	0.0191(6)
C12A	0.0346(2)	0.23457(19)	0.1984(2)	0.0238(7)
C13A	0.1021(2)	0.2070(2)	0.1865(2)	0.0293(8)
C14A	0.1710(3)	0.2531(2)	0.2037(3)	0.0347(9)
C15A	0.1696(2)	0.3242(2)	0.2333(3)	0.0312(8)
N2A	0.99122(18)	0.47600(16)	0.23223(18)	0.0228(6)
C21A	0.9312(2)	0.42293(18)	0.2211(2)	0.0214(6)
C22A	0.8467(2)	0.4469(2)	0.1875(2)	0.0282(8)
C23A	0.8231(3)	0.5202(2)	0.1630(3)	0.0341(9)
C24A	0.8849(3)	0.5709(2)	0.1706(3)	0.0361(9)
C25A	0.9676(2)	0.5477(2)	0.2059(3)	0.0310(8)
B1A	0.9530(2)	0.3346(2)	0.2439(2)	0.0183(7)
O3A	0.87658(14)	0.28950(13)	0.18597(15)	0.0215(5)
C3A	0.8493(2)	0.2961(2)	0.0973(2)	0.0292(8)
C31A	0.9675(2)	0.31368(17)	0.3412(2)	0.0182(6)
C32A	0.9773(2)	0.2281(2)	0.3576(2)	0.0282(7)
C33A	0.0404(3)	0.2187(2)	0.4495(3)	0.0383(9)
C34A	0.1051(2)	0.2803(3)	0.4603(3)	0.0396(10)
C35A	0.0492(2)	0.3484(2)	0.4149(2)	0.0274(7)
C36A	0.0183(3)	0.3941(2)	0.4690(2)	0.0358(9)
C37A	0.9294(3)	0.4176(2)	0.4087(3)	0.0369(9)
C38A	0.8942(2)	0.3443(2)	0.3585(2)	0.0290(8)
Na2	0.76639(9)	0.23432(8)	0.20471(9)	0.0268(3)
Pt2	0.60221(2)	0.32020(2)	0.24970(2)	0.02595(4)
O1B	0.5899(2)	0.21173(16)	0.21396(19)	0.0433(8)

	x/a	y/b	z/c	U(eq)
C1B	0.5381(3)	0.1992(2)	0.1285(3)	0.0416(10)
O2B	0.67717(16)	0.33139(17)	0.19103(17)	0.0342(6)
C2B	0.6393(2)	0.3722(3)	0.1151(3)	0.0360(9)
N1B	0.5264(2)	0.30098(16)	0.30555(19)	0.0262(6)
C11B	0.4678(2)	0.35189(19)	0.3043(2)	0.0225(7)
C12B	0.4127(3)	0.3294(2)	0.3386(2)	0.0292(8)
C13B	0.4170(3)	0.2588(2)	0.3726(3)	0.0399(10)
C14B	0.4782(3)	0.2097(2)	0.3735(3)	0.0449(11)
C15B	0.5309(3)	0.2322(2)	0.3400(3)	0.0382(9)
N2B	0.61805(18)	0.42822(18)	0.28518(19)	0.0253(6)
C21B	0.5536(2)	0.47113(19)	0.2849(2)	0.0218(7)
C22B	0.5695(2)	0.5479(2)	0.3019(2)	0.0288(8)
C23B	0.6476(3)	0.5792(3)	0.3205(3)	0.0417(10)
C24B	0.7119(3)	0.5332(3)	0.3229(3)	0.0491(12)
C25B	0.6950(2)	0.4591(3)	0.3040(3)	0.0401(10)
B1B	0.4601(2)	0.4366(2)	0.2658(2)	0.0188(7)
O3B	0.42348(14)	0.48629(13)	0.31105(14)	0.0209(5)
C3B	0.4698(2)	0.4917(2)	0.4001(2)	0.0256(7)
C31B	0.3914(2)	0.44108(19)	0.1644(2)	0.0200(6)
C32B	0.3000(2)	0.4268(3)	0.1525(2)	0.0367(9)
C33B	0.2559(3)	0.3795(3)	0.0732(3)	0.0484(12)
C34B	0.3278(3)	0.3282(3)	0.0782(3)	0.0531(13)
C35B	0.4044(2)	0.3817(2)	0.1054(2)	0.0323(8)
C36B	0.4097(3)	0.4247(3)	0.0338(3)	0.0445(11)
C37B	0.4443(3)	0.4988(3)	0.0715(3)	0.0448(11)
C38B	0.3948(3)	0.5164(2)	0.1219(3)	0.0343(9)
C1M	0.7651(3)	0.1616(3)	0.3773(3)	0.0421(10)
O1M	0.73376(18)	0.14689(15)	0.28921(17)	0.0318(6)
C2M	0.3237(3)	0.6283(3)	0.4764(3)	0.0376(9)
O2M	0.27604(16)	0.62984(14)	0.38709(15)	0.0259(5)
O1S	0.9361(8)	0.4445(8)	0.9546(7)	0.120(4)
C1S	0.9836(10)	0.4467(8)	0.0365(8)	0.060(2)
C2S	0.0651(10)	0.4876(10)	0.0571(12)	0.067(2)
C3S	0.0343(13)	0.5401(11)	0.9818(13)	0.107(2)
C4S	0.9435(12)	0.5147(14)	0.9354(14)	0.094(2)

Table 4. Bond lengths (Å) for UM2369.

Na1-O1A	2.288(3)	Na1-O3B	2.338(3)
Na1-O1M	2.364(3)	Na1-O2M	2.494(3)
Na1-C3B	2.949(4)	Na1-Pt1	3.4085(14)
Na1-Na2	3.705(2)	Pt1-N2A	2.018(3)
Pt1-O1A	2.018(2)	Pt1-N1A	2.020(3)
Pt1-O2A	2.020(2)	O1A-C1A	1.400(5)
C1A-H1A1	0.98	C1A-H1A2	0.98
C1A-H1A3	0.98	O2A-C2A	1.421(5)
C2A-H2A1	0.98	C2A-H2A2	0.98
C2A-H2A3	0.98	N1A-C15A	1.353(4)
N1A-C11A	1.372(4)	C11A-C12A	1.400(5)
C11A-B1A	1.644(5)	C12A-C13A	1.384(5)
C12A-H12A	0.95	C13A-C14A	1.384(5)
C13A-H13A	0.95	C14A-C15A	1.379(5)
C14A-H14A	0.95	C15A-H15A	0.95
N2A-C25A	1.364(4)	N2A-C21A	1.366(4)
C21A-C22A	1.401(5)	C21A-B1A	1.630(5)
C22A-C23A	1.384(5)	C22A-H22A	0.95
C23A-C24A	1.373(6)	C23A-H23A	0.95
C24A-C25A	1.368(5)	C24A-H24A	0.95
C25A-H25A	0.95	B1A-O3A	1.511(4)
B1A-C31A	1.665(5)	O3A-C3A	1.426(4)
O3A-Na2	2.324(3)	C3A-Na2	3.066(4)
C3A-H3A1	0.98	C3A-H3A2	0.98
C3A-H3A3	0.98	C31A-C32A	1.550(5)
C31A-C38A	1.551(5)	C31A-C35A	1.576(5)
C32A-C33A	1.516(6)	C32A-H32A	0.99
C32A-H32B	0.99	C33A-C34A	1.532(6)
C33A-H33A	0.99	C33A-H33B	0.99
C34A-C35A	1.546(5)	C34A-H34A	0.99
C34A-H34B	0.99	C35A-C36A	1.530(5)
C35A-H35A	1.0	C36A-C37A	1.509(6)
C36A-H36A	0.99	C36A-H36B	0.99
C37A-C38A	1.548(6)	C37A-H37A	0.99
C37A-H37B	0.99	C38A-H38A	0.99
C38A-H38B	0.99	Na2-O2B	2.278(3)
Na2-O3A	2.324(3)	Na2-O2M	2.365(3)

Na2-O1M	2.399(3)	Na2-C3A	3.066(4)
Na2-Pt2	3.6534(14)	Na2-Na1	3.705(2)
Pt2-N1B	2.009(3)	Pt2-N2B	2.009(3)
Pt2-O2B	2.015(3)	Pt2-O1B	2.019(3)
O1B-C1B	1.393(5)	C1B-H1B1	0.98
C1B-H1B2	0.98	C1B-H1B3	0.98
O2B-C2B	1.407(5)	C2B-H2B1	0.98
C2B-H2B2	0.98	C2B-H2B3	0.98
N1B-C15B	1.358(5)	N1B-C11B	1.367(4)
C11B-C12B	1.408(5)	C11B-B1B	1.639(5)
C12B-C13B	1.384(5)	C12B-H12B	0.95
C13B-C14B	1.383(7)	C13B-H13B	0.95
C14B-C15B	1.363(6)	C14B-H14B	0.95
C15B-H15B	0.95	N2B-C25B	1.358(5)
N2B-C21B	1.366(4)	C21B-C22B	1.406(5)
C21B-B1B	1.645(5)	C22B-C23B	1.381(5)
C22B-H22B	0.95	C23B-C24B	1.383(6)
C23B-H23B	0.95	C24B-C25B	1.365(6)
C24B-H24B	0.95	C25B-H25B	0.95
B1B-O3B	1.515(4)	B1B-C31B	1.660(5)
O3B-C3B	1.418(4)	C3B-H3B1	0.98
C3B-H3B2	0.98	C3B-H3B3	0.98
C31B-C32B	1.546(5)	C31B-C38B	1.555(5)
C31B-C35B	1.573(5)	C32B-C33B	1.521(6)
C32B-H32C	0.99	C32B-H32D	0.99
C33B-C34B	1.531(7)	C33B-H33C	0.99
C33B-H33D	0.99	C34B-C35B	1.543(6)
C34B-H34C	0.99	C34B-H34D	0.99
C35B-C36B	1.517(6)	C35B-H35B	1.0
C36B-C37B	1.485(7)	C36B-H36C	0.99
C36B-H36D	0.99	C37B-C38B	1.528(6)
C37B-H37C	0.99	C37B-H37D	0.99
C38B-H38C	0.99	C38B-H38D	0.99
C1M-O1M	1.427(5)	C1M-H1M1	0.98
C1M-H1M2	0.98	C1M-H1M3	0.98
O1M-Na1	2.364(3)	O1M-H1M	0.84
C2M-O2M	1.421(5)	C2M-H2M1	0.98
C2M-H2M2	0.98	C2M-H2M3	0.98

O2M-Na2	2.365(3)	O2M-H2M	0.84
O1S-C1S	1.311(16)	O1S-C4S	1.322(17)
C1S-C2S	1.502(9)	C2S-C3S	1.518(10)
C3S-C4S	1.504(9)		

Crystal structure determination for H[1]·HCl

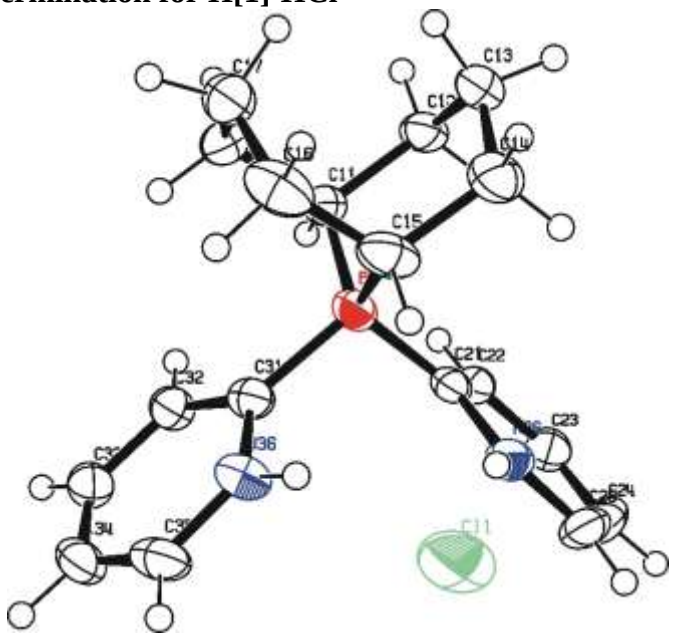

A colorless prism-like specimen of $C_{18}H_{24}BClN_2O_{0.42}$, approximate dimensions 0.14 mm × 0.26 mm × 0.43 mm, was used for the X-ray crystallographic analysis. The X-ray intensity data were measured on a Bruker APEX-II CCD system equipped with a graphite monochromator and a MoKα sealed tube (λ = 0.71073 Å). Data collection temperature was 100 K.

The total exposure time was 33.67 hours. The frames were integrated with the Bruker SAINT software package using a narrow-frame algorithm. The integration of the data using a triclinic unit cell yielded a total of 6145 reflections to a maximum θ angle of 25.00° (0.84 Å resolution), of which 6145 were independent (average redundancy 1.000, completeness = 99.7%) and 5548 (90.28%) were greater than $2\sigma(F^2)$. The final cell constants of a = 8.4357(8) Å, b = 13.7411(14) Å, c = 15.5693(15) Å, α = 79.680(2)°, β = 80.340(2)°, γ = 89.731(2)°, V = 1749.8(3) Å^3, are based upon the refinement of the XYZ-centroids of 3978 reflections above 20 σ(I) with 5.685° < 2θ < 55.51°. Data were corrected for absorption effects using the multi-scan method (SADABS). The structure was solved and refined using the Bruker SHELXTL Software Package, with Z = 4 for the formula unit, $C_{18}H_{24}BClN_2O_{0.42}$. The final anisotropic full-matrix least-squares refinement on F^2 with 564 variables converged at R_1 = 4.70%, for the observed data and wR_2 = 9.42% for all data. The goodness-of-fit was 1.000. The largest peak in the final difference electron density synthesis was 0.597 e^-/Å^3 and the largest hole was -0.628 e^-/Å^3 with an RMS deviation of 0.040 e^-/Å^3. On the basis of the final model, the calculated density was 1.220 g/cm^3 and F(000), 685 e^-

.

APEX2 Version 2010.11-3 (Bruker AXS Inc.)
SAINT Version 7.68A (Bruker AXS Inc., 2009)
SADABS Version 2008/1 (G. M. Sheldrick, Bruker AXS Inc.)
XPREP Version 2008/2 (G. M. Sheldrick, Bruker AXS Inc.)
XS Version 2008/1 (G. M. Sheldrick, *Acta Cryst.* (2008). A**64**, 112-122)
XL Version 2008/4 (G. M. Sheldrick, *Acta Cryst.* (2008). A**64**, 112-122)
Platon (A. L. Spek, *Acta Cryst.* (1990). A**46**, C-34)

Table 1. Sample and crystal data for UM2326.

Identification code	2326	
Chemical formula	$C_{18}H_{24}BClN_2O_{0.42}$	
Formula weight	321.37	
Temperature	100(2) K	
Wavelength	0.71073 Å	
Crystal size	0.14 × 0.26 × 0.43 mm	
Crystal habit	colorless prism	
Crystal system	triclinic	
Unit cell dimensions	a = 8.4357(8) Å	α = 79.680(2)°
	b = 13.7411(14) Å	β = 80.340(2)°
	c = 15.5693(15) Å	γ = 89.731(2)°
Volume	1749.8(3) $Å^3$	
Z	4	
Density (calculated)	1.220 Mg/cm^3	
Absorption coefficient	0.219 mm^{-1}	
F(000)	685	

Table 2. Data collection and structure refinement for UM2326.

Diffractometer	Bruker APEX-II CCD	
Radiation source	sealed tube, MoKα	
Theta range for data collection	2.20 to 25.00°	
Reflections collected	6145	
Coverage of independent reflections	99.7%	
Absorption correction	multi-scan	
Structure solution technique	direct methods	
Structure solution program	SHELXS-97 (Sheldrick, 2008)	
Refinement method	Full-matrix least-squares on F^2	
Refinement program	SHELXL-2012	
Function minimized	$\Sigma\, w(F_o^2 - F_c^2)^2$	
Data / restraints / parameters	6145 / 295 / 564	
Goodness-of-fit on F^2	1.000	
Final R indices	5548 data; I>2σ(I)	R_1 = 0.0470, wR_2 = 0.0915
	all data	R_1 = 0.0531, wR_2 = 0.0942
Weighting scheme	$w=1/[\sigma^2(F_o^2)+(0.0100P)^2+1.3840P]$, $P=(F_o^2+2F_c^2)/3$	
Largest diff. peak and hole	0.597 and -0.628 eÅ^{-3}	
R.M.S. deviation from mean	0.040 eÅ^{-3}	

$R_1 = \Sigma||F_o| - |F_c|| / \Sigma|F_o|$
$GOOF = S = \{\Sigma[w(F_o^2 - F_c^2)^2] / (n - p)\}^{1/2}$
$wR_2 = \{\Sigma[w(F_o^2 - F_c^2)^2] / \Sigma[w(F_o^2)^2]\}^{1/2}$

Table 3. Atomic coordinates and equivalent isotropic atomic displacement parameters (Å^2) for UM2326.

U(eq) is defined as one third of the trace of the orthogonalized U_{ij} tensor.

	x/a	y/b	z/c	U(eq)
Cl1	0.38583(11)	0.87965(7)	0.45787(4)	0.0734(3)
Cl2	0.63782(12)	0.43029(12)	0.34063(12)	0.0514(4)
Cl2A	0.6304(3)	0.3880(3)	0.3780(3)	0.0514(4)
O1A	0.3710(7)	0.4172(4)	0.5332(3)	0.061(2)
O2A	0.4275(5)	0.3216(3)	0.5037(3)	0.0485(16)
B1	0.3391(3)	0.9483(2)	0.18817(15)	0.0314(5)
C11	0.2806(2)	0.97250(16)	0.09207(13)	0.0298(5)
C12	0.1776(3)	0.06584(17)	0.08654(16)	0.0367(6)
C13	0.0339(3)	0.06288(19)	0.16166(17)	0.0425(6)
C14	0.0721(3)	0.0218(2)	0.25366(18)	0.0500(7)
C15	0.1719(3)	0.9267(2)	0.25997(15)	0.0420(6)
C16	0.0822(3)	0.8356(2)	0.24293(18)	0.0479(7)
C17	0.0486(3)	0.84136(19)	0.14880(17)	0.0426(6)
C18	0.1900(3)	0.88202(18)	0.07621(16)	0.0363(5)
C21	0.4530(3)	0.03739(17)	0.20518(15)	0.0331(5)
C22	0.5417(3)	0.10820(18)	0.13992(16)	0.0361(6)
C23	0.6398(3)	0.1784(2)	0.16007(18)	0.0473(7)
C24	0.6525(3)	0.1782(2)	0.2479(2)	0.0587(9)
C25	0.5694(3)	0.1078(2)	0.3115(2)	0.0587(9)
N26	0.4737(3)	0.04169(17)	0.28904(14)	0.0446(6)
C31	0.4599(3)	0.85398(16)	0.19506(15)	0.0302(5)
C32	0.5564(3)	0.82170(17)	0.12438(16)	0.0332(5)
C33	0.6566(3)	0.74248(18)	0.13674(17)	0.0380(6)
C34	0.6640(3)	0.69317(18)	0.22127(18)	0.0416(6)
C35	0.5747(3)	0.72644(19)	0.29098(18)	0.0427(6)
N36	0.4764(2)	0.80340(15)	0.27638(13)	0.0363(5)
B2	0.1691(5)	0.4369(3)	0.2519(3)	0.0290(6)
C41	0.3465(4)	0.4687(3)	0.1915(3)	0.0305(10)
C42	0.3348(7)	0.5719(3)	0.1336(4)	0.0380(11)
C43	0.2010(10)	0.5817(11)	0.0765(8)	0.0403(8)
C44	0.0392(9)	0.5333(4)	0.1245(5)	0.0359(12)
C45	0.0484(6)	0.4310(4)	0.1823(4)	0.0338(11)
C46	0.1106(6)	0.3485(3)	0.1298(3)	0.0365(10)
C47	0.2862(7)	0.3591(4)	0.0834(3)	0.0435(15)

	x/a	y/b	z/c	U(eq)
C48	0.4048(6)	0.3880(4)	0.1396(3)	0.0446(11)
C51	0.1180(8)	0.5147(13)	0.3219(11)	0.0239(13)
C52	0.2213(5)	0.5630(3)	0.3625(2)	0.0321(9)
C53	0.1635(8)	0.6234(7)	0.4221(5)	0.0379(19)
C54	0.9993(7)	0.6362(5)	0.4432(4)	0.0389(14)
C55	0.8981(5)	0.5873(3)	0.4054(2)	0.0337(9)
N56	0.9597(5)	0.5295(3)	0.3471(3)	0.0275(9)
C61	0.1722(6)	0.3335(4)	0.3258(3)	0.0258(10)
C62	0.0414(6)	0.2683(3)	0.3584(3)	0.0331(10)
C63	0.0468(6)	0.1868(4)	0.4250(4)	0.0433(15)
C64	0.1860(6)	0.1688(4)	0.4601(3)	0.0497(14)
C65	0.3138(5)	0.2330(3)	0.4294(3)	0.0448(11)
N66	0.3038(3)	0.3113(2)	0.36375(18)	0.0324(8)
B2A	0.1577(3)	0.4277(2)	0.25480(18)	0.0290(6)
C41A	0.3162(3)	0.4242(2)	0.18502(18)	0.0324(15)
C42A	0.3550(10)	0.5317(4)	0.1306(5)	0.0380(11)
C43A	0.2197(14)	0.5749(16)	0.0809(12)	0.0403(8)
C44A	0.0512(13)	0.5583(6)	0.1371(7)	0.0359(12)
C45A	0.0164(9)	0.4535(6)	0.1932(5)	0.0338(11)
C46A	0.0041(8)	0.3749(4)	0.1336(4)	0.0338(13)
C47A	0.1632(8)	0.3557(4)	0.0756(4)	0.0323(14)
C48A	0.3073(8)	0.3496(5)	0.1244(4)	0.0303(16)
C51A	0.1509(13)	0.503(2)	0.3221(17)	0.0239(13)
C52A	0.0180(8)	0.5503(6)	0.3595(5)	0.0302(16)
C53A	0.0277(9)	0.6098(6)	0.4215(5)	0.0301(17)
C54A	0.1734(9)	0.6211(10)	0.4495(7)	0.033(2)
C55A	0.3017(6)	0.5716(4)	0.4149(3)	0.0338(13)
N56A	0.2876(6)	0.5167(4)	0.3538(3)	0.0276(11)
C61A	0.1154(7)	0.3203(5)	0.3187(5)	0.0258(10)
C62A	0.2318(6)	0.2588(4)	0.3512(3)	0.0279(12)
C63A	0.1904(8)	0.1746(4)	0.4146(4)	0.0375(16)
C64A	0.0296(8)	0.1490(5)	0.4466(6)	0.040(2)
C65A	0.9164(7)	0.2109(4)	0.4162(3)	0.0384(14)
N66A	0.9617(6)	0.2928(4)	0.3555(3)	0.0269(11)

Table 3. Atomic coordinates and equivalent isotropic atomic

displacement parameters (Å^2) for UM2326.

U(eq) is defined as one third of the trace of the orthogonalized U_{ij} tensor.

	x/a	y/b	z/c	U(eq)
Cl1	0.38583(11)	0.87965(7)	0.45787(4)	0.0734(3)
Cl2	0.63782(12)	0.43029(12)	0.34063(12)	0.0514(4)
Cl2A	0.6304(3)	0.3880(3)	0.3780(3)	0.0514(4)
O1A	0.3710(7)	0.4172(4)	0.5332(3)	0.061(2)
O2A	0.4275(5)	0.3216(3)	0.5037(3)	0.0485(16)
B1	0.3391(3)	0.9483(2)	0.18817(15)	0.0314(5)
C11	0.2806(2)	0.97250(16)	0.09207(13)	0.0298(5)
C12	0.1776(3)	0.06584(17)	0.08654(16)	0.0367(6)
C13	0.0339(3)	0.06288(19)	0.16166(17)	0.0425(6)
C14	0.0721(3)	0.0218(2)	0.25366(18)	0.0500(7)
C15	0.1719(3)	0.9267(2)	0.25997(15)	0.0420(6)
C16	0.0822(3)	0.8356(2)	0.24293(18)	0.0479(7)
C17	0.0486(3)	0.84136(19)	0.14880(17)	0.0426(6)
C18	0.1900(3)	0.88202(18)	0.07621(16)	0.0363(5)
C21	0.4530(3)	0.03739(17)	0.20518(15)	0.0331(5)
C22	0.5417(3)	0.10820(18)	0.13992(16)	0.0361(6)
C23	0.6398(3)	0.1784(2)	0.16007(18)	0.0473(7)
C24	0.6525(3)	0.1782(2)	0.2479(2)	0.0587(9)
C25	0.5694(3)	0.1078(2)	0.3115(2)	0.0587(9)
N26	0.4737(3)	0.04169(17)	0.28904(14)	0.0446(6)
C31	0.4599(3)	0.85398(16)	0.19506(15)	0.0302(5)
C32	0.5564(3)	0.82170(17)	0.12438(16)	0.0332(5)
C33	0.6566(3)	0.74248(18)	0.13674(17)	0.0380(6)
C34	0.6640(3)	0.69317(18)	0.22127(18)	0.0416(6)
C35	0.5747(3)	0.72644(19)	0.29098(18)	0.0427(6)
N36	0.4764(2)	0.80340(15)	0.27638(13)	0.0363(5)
B2	0.1691(5)	0.4369(3)	0.2519(3)	0.0290(6)
C41	0.3465(4)	0.4687(3)	0.1915(3)	0.0305(10)
C42	0.3348(7)	0.5719(3)	0.1336(4)	0.0380(11)
C43	0.2010(10)	0.5817(11)	0.0765(8)	0.0403(8)
C44	0.0392(9)	0.5333(4)	0.1245(5)	0.0359(12)
C45	0.0484(6)	0.4310(4)	0.1823(4)	0.0338(11)
C46	0.1106(6)	0.3485(3)	0.1298(3)	0.0365(10)
C47	0.2862(7)	0.3591(4)	0.0834(3)	0.0435(15)
C48	0.4048(6)	0.3880(4)	0.1396(3)	0.0446(11)

	x/a	y/b	z/c	U(eq)
C51	0.1180(8)	0.5147(13)	0.3219(11)	0.0239(13)
C52	0.2213(5)	0.5630(3)	0.3625(2)	0.0321(9)
C53	0.1635(8)	0.6234(7)	0.4221(5)	0.0379(19)
C54	0.9993(7)	0.6362(5)	0.4432(4)	0.0389(14)
C55	0.8981(5)	0.5873(3)	0.4054(2)	0.0337(9)
N56	0.9597(5)	0.5295(3)	0.3471(3)	0.0275(9)
C61	0.1722(6)	0.3335(4)	0.3258(3)	0.0258(10)
C62	0.0414(6)	0.2683(3)	0.3584(3)	0.0331(10)
C63	0.0468(6)	0.1868(4)	0.4250(4)	0.0433(15)
C64	0.1860(6)	0.1688(4)	0.4601(3)	0.0497(14)
C65	0.3138(5)	0.2330(3)	0.4294(3)	0.0448(11)
N66	0.3038(3)	0.3113(2)	0.36375(18)	0.0324(8)
B2A	0.1577(3)	0.4277(2)	0.25480(18)	0.0290(6)
C41A	0.3162(3)	0.4242(2)	0.18502(18)	0.0324(15)
C42A	0.3550(10)	0.5317(4)	0.1306(5)	0.0380(11)
C43A	0.2197(14)	0.5749(16)	0.0809(12)	0.0403(8)
C44A	0.0512(13)	0.5583(6)	0.1371(7)	0.0359(12)
C45A	0.0164(9)	0.4535(6)	0.1932(5)	0.0338(11)
C46A	0.0041(8)	0.3749(4)	0.1336(4)	0.0338(13)
C47A	0.1632(8)	0.3557(4)	0.0756(4)	0.0323(14)
C48A	0.3073(8)	0.3496(5)	0.1244(4)	0.0303(16)
C51A	0.1509(13)	0.503(2)	0.3221(17)	0.0239(13)
C52A	0.0180(8)	0.5503(6)	0.3595(5)	0.0302(16)
C53A	0.0277(9)	0.6098(6)	0.4215(5)	0.0301(17)
C54A	0.1734(9)	0.6211(10)	0.4495(7)	0.033(2)
C55A	0.3017(6)	0.5716(4)	0.4149(3)	0.0338(13)
N56A	0.2876(6)	0.5167(4)	0.3538(3)	0.0276(11)
C61A	0.1154(7)	0.3203(5)	0.3187(5)	0.0258(10)
C62A	0.2318(6)	0.2588(4)	0.3512(3)	0.0279(12)
C63A	0.1904(8)	0.1746(4)	0.4146(4)	0.0375(16)
C64A	0.0296(8)	0.1490(5)	0.4466(6)	0.040(2)
C65A	0.9164(7)	0.2109(4)	0.4162(3)	0.0384(14)
N66A	0.9617(6)	0.2928(4)	0.3555(3)	0.0269(11)

F. References

1) J.D. Scott, R.J. Puddephatt, *Organometallics* **1983**, *2*, 1643-1648.

2) C. Cui, *Doc. Dissertation Res.*, **2010**, Newark Rutgers- The State University of New Jersey.

3) R.G. Parr, W. Yang, *Density-functional Theory of Atoms and Molecules*; Oxford University Press: Oxford, 1989.

4) J.P. Perdew, K. Burke, M. Ernzerhof, *Phys. Rev. Lett.* **1996**, *77*, 3865-3868.

5) Jaguar, version 7.9, Schrödinger, LLC, New York, NY, 2012.

6) *CRC Handbook of Chemistry and Physics*, 92nd Ed, 2011.

7) a) K. Fischer, M. Wilken, *J. Chem. Thermodynamics* **2001**, 33, 1285–1308; b) C.B. Kretschmer, J. Nowakowska, R. Wiebe, *Ind. Eng. Chem.* **1946**, *38*, 506-509.

8) C.P. Kelly, C.J. Cramer, D.G. Truhlar, *J. Phys. Chem. B* 2007, *111*, 408-422.